



## Strings as Multi-Particle States of Quantum Sigma-Models

Nikolay Gromov<sup>a,b,c</sup>, Vladimir Kazakov<sup>a,b,\*</sup>, Kazuhiro Sakai<sup>a,†</sup>, Pedro Vieira<sup>a,b,d</sup>

<sup>a</sup> *Laboratoire de Physique Théorique  
de l'Ecole Normale Supérieure<sup>‡</sup> et <sup>b</sup> l'Université Paris-VI,  
Paris, 75231, France<sup>§</sup>*

<sup>c</sup> *St.Petersburg INP,  
Gatchina, 188 300, St.Petersburg, Russia*

<sup>d</sup> *Departamento de Física e Centro de Física do Porto  
Faculdade de Ciências da Universidade do Porto  
Rua do Campo Alegre, 687, 4169-007 Porto, Portugal*

### ABSTRACT

We study the quantum Bethe ansatz equations in the  $O(2n)$  sigma-model for physical particles on a circle, with the interaction given by the Zamolodchikovs' S-matrix, in view of its application to quantization of the string on the  $S^{2n-1} \times R_t$  space. For a finite number of particles, the system looks like an inhomogeneous integrable  $O(2n)$  spin chain. Similarly to  $OSp(2m+n|2m)$  conformal sigma-model considered by Mann and Polchinski, we reproduce in the limit of large density of particles the finite gap Kazakov–Marshakov–Minahan–Zarembo solution for the classical string and its generalization to the  $S^5 \times R_t$  sector of the Green–Schwarz–Metsaev–Tseytlin superstring. We also reproduce some quantum effects: the BMN limit and the quantum homogeneous spin chain similar to the one describing the bosonic sector of the one-loop  $\mathcal{N} = 4$  super Yang–Mills theory. We discuss the prospects of generalization of these Bethe equations to the full superstring sigma-model.

---

\*Membre de l'Institut Universitaire de France

†Chercheur Associé du C.N.R.S.

‡Unité mixte du C.N.R.S. et de l' Ecole Normale Supérieure, UMR 8549.

§gromov@thd.pmpi.spb.ru, kazakov@physique.ens.fr, sakai@lpt.ens.fr, pedro@lpt.ens.fr

## Contents

<b>1</b>	<b>Introduction</b>	<b>2</b>
<b>2</b>	<b><math>O(2n)</math> Sigma-Model and Classically Integrable String Theory</b>	<b>6</b>
2.1	Definition of the Sigma-Model on $S^{2n-1}$ and Virasoro Conditions . . . . .	6
2.2	Classical Integrability and Finite Gap Solution . . . . .	7
2.3	Classical $SU(2)$ Principal Chiral Field . . . . .	9
2.4	Definition of the Model . . . . .	9
<b>3</b>	<b>Quantum Bethe Ansatz and Classical Limit: <math>O(4)</math> Sigma-Model</b>	<b>11</b>
3.1	Bethe Equations for Particles on a Circle . . . . .	12
3.2	The Classical Limit . . . . .	13
3.3	Highest Weight States of $U(1)$ Sector in Classical Limit . . . . .	16
3.4	General Classical States and Its Algebraic Curve . . . . .	19
3.5	Energy and Momentum . . . . .	20
<b>4</b>	<b>Matching with the Finite Gap KMMZ Solution</b>	<b>22</b>
<b>5</b>	<b>Some Limiting Solutions of the Quantum <math>O(n)</math> Sigma-Model</b>	<b>25</b>
5.1	BMN Limit . . . . .	25
5.2	Multi Cut Vacuum States . . . . .	26
5.3	XXX Spin Chain Limit . . . . .	28
<b>6</b>	<b><math>O(6)</math> Sigma-Model</b>	<b>30</b>
6.1	Algebraic Curve . . . . .	31
6.1.1	Curve for the Vector Representation . . . . .	31
6.1.2	Curve for the Spinor Representation . . . . .	34
6.2	Energy and Momentum . . . . .	36
<b>7</b>	<b>Conclusions and Prospects</b>	<b>36</b>
	<b>Appendix A Charged Particles in a Box</b>	<b>38</b>
	<b>Appendix B Relating resolvents</b>	<b>39</b>
	<b>Appendix C Bootstrap and Bethe Ansatz</b>	<b>40</b>
	<b>Appendix D Bethe Ansatz Equations for <math>O(2n)</math> Sigma-Model</b>	<b>45</b>

## 1 Introduction

Superstring theory on non-trivial gravitational backgrounds is extremely important for the progress of the theory of fundamental interactions and cosmology: not only it might describe some rather realistic models in cosmology and black hole physics but it also provides a dual description of some strongly interacting planar Yang–Mills gauge theories. A set of these dualities are often named as AdS/CFT correspondence [1–3] (see [4] for the review). Apart from its physical significance for the strongly interacting gauge theories a great technical advantage of the string side of duality is that the string theory in the tree approximation is a two dimensional  $\sigma$ -model, at least in the world-sheet perturbation theory, and the string interactions are not relevant in the planar 't Hooft limit of the dual gauge theory. And since the two-dimensional  $\sigma$ -models are sometimes solvable it gives us hopes that so are some realistic string sigma-models, together with the dual supersymmetric Yang–Mills (SYM) theories in the large  $N$  limit.

The master-example of the AdS/CFT correspondence, the 4-dimensional conformal  $\mathcal{N} = 4$  SYM theory, and its dual, the Green–Schwarz–Metsaev–Tseytlin superstring [5] on the  $AdS_5 \times S^5$  background looks particularly promising in this respect. The 1-loop integrability was discovered in  $\mathcal{N} = 4$  SYM in [6] for the bosonic sector<sup>1</sup> where the dilatation operator was identified with the Hamiltonian of an integrable 1-dimensional spin chain. It was soon followed by the demonstration of the classical integrability of the full superstring  $\sigma$ -model on  $AdS_5 \times S^5$  [9], where already some exact particular classical string solutions were known [10–12]. It was then shown in [13] that the integrability might persist in  $\mathcal{N} = 4$  SYM even in higher loops, and is certainly a property of the full theory at one loop [14, 15]. The underlying (super) spin chains are solvable by the standard Bethe ansatz technique and possess an interesting ferromagnetic continuous limit [16–18] corresponding to very long local single trace operators in SYM. The resulting anomalous dimensions were directly compared for some states with the energies of classical string solutions in the so called Frolov–Tseytlin limit.

As a next step in this progress, the general classical solution for the superstring rotating on  $AdS_5 \times S^5$  was proposed, first for the  $S^3 \times R_t$  sector [19], then for  $AdS_3 \times S^1$  [20],  $S^5 \times R_t$  [21], and finally for the full  $AdS_5 \times S^5$  superstring [22]. The full solution even bears an imprint of fermions in the corresponding algebraic curve describing a finite gap solution. It was shown in [19, 21, 23, 24] that *all* states and anomalous dimensions of the SYM theory can be mapped onto *all* classical states of the string in this particular limit, giving another impressive demonstration of the AdS/CFT correspondence.

This integrability is recently generalized to three-loops [14, 25] and even a plausible perturbative all-loop ansatz was proposed [26, 27]. The perturbative comparison of the AdS/CFT correspondence works well for this ansatz up to two loops but breaks down at three loops [28], a mismatch usually explained by certain non-perturbative effects which are difficult to take into account in the comparison of the weak and strong coupling regimes.<sup>2</sup> One-loop world-sheet

---

<sup>1</sup>Integrable spin chains have been discovered in (non-supersymmetric) gauge theories before [7, 8].

<sup>2</sup>Nevertheless, the classical string KMMZ solution [19] inspired a beautiful result of [25], where the three-loop

calculations for particular string solutions [29], as well as the direct one-loop world-sheet calculation of the BMN spectra [30–32] also show a perfect AdS/CFT correspondence with respect to similar quantum corrections to the solutions in SYM spin chains in the scaling limit [33–36].

In spite of the multitude of signs of integrability of the  $\mathcal{N} = 4$  SYM, the ultimate progress is hardly possible without the establishment of integrability of the full quantum string  $\sigma$ -model. It is not an easy task, though far from being hopeless (see a discussion in [37]). Similar  $\sigma$ -models were already proven to be integrable starting from the Zamolodchikovs’ discovery of the factorized unitary and crossing-invariant S-matrix for physical particles in the  $O(n)$  sigma-model [38]. Then the  $SU(n)_L \times SU(n)_R$  principal chiral field was solved [39–44] and the corresponding physical S-matrix was found [40]. This model represents the first non-trivial example of the field theory completely solvable in the ’t Hooft limit [45]. Some supersymmetric  $\sigma$ -models, including conformal ones, appeared to be integrable as well [46–48].

The main difficulties for establishing the integrability of the full superstring are the following:

1. It is a non-compact  $\sigma$ -model as the  $AdS_5$  subspace is. The S-matrix approach is complicated by the existence of a continuous spectrum of asymptotic states, although we know some integrable  $\sigma$ -models of this kind: quantum Liouville theory [49–52] bearing many similarities with a coset of  $AdS_3$  sigma-model [53], the Sine-Liouville theory and its strong-coupling dual, the 2D dilatonic black hole <sup>3</sup>.

2. The Virasoro conditions impose a complicated selection rule on the possible quantum states: they eliminate the longitudinal motions of the string forbidden by the world-sheet reparametrization symmetry, together with the corresponding quantum states. We could start from a gauge which eliminates the conformal redundancy from the beginning, but it hides the world-sheet Lorentz covariance as well.

3. It seems hopeless to find a completely closed subsector of the superstring on  $AdS_5 \times S^5$  at the quantum mechanical and nonperturbative level, and to write down a selfconsistent system of Bethe equations for it (though see some instructive attempts in [58–60]). To obtain the right divergency free string sigma model we have to consider the full theory, including fermions.

The full Metsaev–Tseytlin superstring looks like two sigma models, one on  $AdS_5$ , another on  $S^5$  space, each containing 4 on-shell bosonic fields “glued” together by 16 fermionic fields (8 on-shell fields). Classically the fermions do not influence the dynamics and the system looks like two independent bosonic  $\sigma$ -models. If we quantize the  $S^5$   $\sigma$ -model (with a trivial inclusion of the  $AdS$ -time coordinate, which makes it  $S^5 \times R_t$ ) it will show the asymptotically free behavior, even if we impose the analogue of Virasoro constraints (no longitudinal modes). Nevertheless, this compact  $O(6)$   $\sigma$ -model may provide a valuable information on the full superstring: its classical limit describes precisely the compact sector of the superstring [21] and its quantization should bear some important features of the full quantum superstring  $\sigma$ -model. And if we manage to

---

dilatation operator was constructed for some subsectors of  $N=4$  SYM.

<sup>3</sup>Similarly to the AdS/CFT correspondence of superstring to the SYM, they also have their dual, matrix models and matrix quantum mechanics description for the  $c = 1$  matrix model [54], or the matrix black hole model of [55] (see [56] for the discussion of this issue).

impose the Virasoro constraints in a natural way it can serve as a rather sophisticated toy model for the quantum superstring.

Our principal motivation in this paper is to study the full quantum version of the  $O(2n)$  sigma model in the context of its application to the string theory. Our starting point is the Zamolodchikovs' S-matrix for physical particles. We put  $L$  such particles on a circle and study possible states by means of the nested Bethe ansatz equations diagonalizing the underlying monodromy matrix by the use of the quantum inverse scattering method [61, 62]. The main result may be interesting not only to the string theorists but also to the specialists in integrable 2D field theories: we reconstruct all finite gap solutions of [19,21] for the classical string motions on  $S^5 \times R_t$ , directly from these Bethe equations in the limit of large density of the particles with sufficiently big momenta. In this limit, the theory is in the extreme asymptotically free regime. We can neglect the conformal anomaly since the particles are almost massless, and the states are classical solitons. These solitons are nothing but the classical string states. The string looks like a collective state of the particles. The string mode numbers can be identified with certain "magnon" mode numbers of the Bethe equations, the number of excited modes corresponds to the number of gaps in finite gap solution (this number is equal to the genus of the algebraic curve describing the solution), and the amplitude of a mode is fixed by the number of Bethe roots forming the corresponding gap.

The system looks like an inhomogeneous  $SO(6)$  spin chain with the nearest neighbor interactions defined by the rapidities of the neighboring particles. The rapidities, in their turn, are fixed from the periodicity condition, thus make the spin chain dynamical<sup>4</sup>.

Qualitatively it is quite similar to the  $OSp(2m+n|2m)$  supersymmetric  $\sigma$ -model of [64], conformal in the limit  $n \rightarrow 2$ . Our way to restore the classical limit is also inspired by [64], but the details are very different, since our model is conformal only classically. However, some features of our model look closer to compact sectors of the string theory on  $AdS_5 \times S^5$ . In particular, in a certain limit we restore the homogeneous spin chain, the same (up to some normalizations) as the one describing the 1-loop SYM theory in the corresponding sector. To make it working for higher SYM loops it might be necessary to incorporate into the future string  $\sigma$ -model certain features of the Hubbard model which is a good candidate for reproducing all loops of the perturbative SYM [65].

The classical string solutions are encoded into an algebraic curve. To each curve with the fixed moduli one can associate the unique (up to some trivial choice of initial conditions, as proven in [66]) classical string solution with Virasoro conditions imposed and with the number of excited oscillatory modes corresponding to the genus of the curve.

The algebraic curve obtained in [19,21] from the purely classical finite gap method [67] turns out to be the same as the one extracted here from the Bethe equations, and the two different

---

<sup>4</sup>Not to confuse it with the dynamical S-matrix of [63] for the  $su(3|2)$  sector of the  $\mathcal{N} = 4$  SYM where even the length of the chain can change, a feature certainly to be taken into account for the full string  $\sigma$ -model.

projections (Riemann surfaces) of the curve are related by Zhukovsky map

$$z = x + 1/x,$$

which is an important part of the construction<sup>5</sup>. It was used already in [19] for the successful 2-loop comparison of the string and SYM results and its significance is better understood in [26,58,66]. This map might identify the right variables to quantize in the full superstring theory.

The Virasoro conditions deserve a special mentioning here. As it will be seen from our classical limit procedure, the correct classical string solutions are related only to Bethe states where all rapidities of the physical particles have the same mode number. In the classical limit they condense into a single cut, which reproduces, after Zhukovsky transformation, the two pole structure of the algebraic curve of the finite gap solution. We conjecture that this is the way to impose the Virasoro-like constraints for any general quantum state as well: the rapidities should have the same mode number. We confirm it by some examples of particular solutions with small longitudinal amplitudes.<sup>6</sup>

Finally, we would like to mention that the Bethe ansatz description provides an unusual example of the holography in the string theory: the Bethe roots look like the positions of some D-branes reducing the quantization procedure to a certain “discretization” of the underlying algebraic curves. But unlike the matrix model description of D-branes where the eigenvalues serve as quantum coordinates of the D-branes and should be dynamical variables, the Bethe roots of the stringy  $\sigma$ -models are fixed by the periodicity condition.

The paper is organized as follows. In section 2, we define the  $O(2n)$   $\sigma$ -model and remind its classical integrability properties allowing the finite gap solution. In section 3, the quantum Bethe ansatz solution of the  $SU(2)$  principal chiral field model, equivalent to the  $O(4)$   $\sigma$ -model, is presented and its classical limit is considered and the corresponding algebraic curve is constructed. In section 4, we map this algebraic curve to the curve of the finite gap solution obtained directly from the classical action, fixing appropriately the relations between all the parameters of two approaches. In section 5, the construction is generalized to the  $O(6)$  sector. In conclusions we make some remarks concerning possible generalizations of this construction to the full superstring on  $AdS_5 \times S^5$  and problems related to it. In Appendix A the solution for the  $U(1)$  sector in the scaling limit is presented in detail. In Appendix B we provide an alternative proof of our correspondence for the  $O(4)$  sector, namely through the transformation of resolvents. In Appendix C both the bootstrap method as well as the algebraic Bethe ansatz

---

<sup>5</sup>The Zhukovsky map was proposed in 1906 in [68] for description of aerodynamics of the airplane wing. It maps a circle passing through the point  $x = 1$  into a wing-shaped figure in  $z$ -plane (see the front page).

<sup>6</sup>At the classical level Virasoro constraints have a clear interpretation as a restriction on the allowed solutions forbidding longitudinal motions of the string, even if we truncate the full  $AdS_5 \times S^5$  theory to a subsector, like the  $S^5 \times R$  subsector considered in this paper. On the quantum level, the subsectors are not even described by a conformal field theory and the Virasoro constraints do not have a clear meaning and are not imposed by the reparametrization symmetry. Therefore we rather have to speak in this case about a natural selection rule for the quantum states which leads to the standard Virasoro conditions in the classical limit.

program are reviewed for the  $O(4)$   $\sigma$ -model. In Appendix D this is generalized to the  $O(2n)$   $\sigma$ -model.

## 2 $O(2n)$ Sigma-Model and Classically Integrable String Theory

The main system of our interest is the superstring on the  $AdS_5 \times S^5$  background. A compact bosonic subsector of it is described by the sigma model on the subspace  $S^5 \times R_t$ , where  $R_t$  is the coordinate corresponding to the AdS time. The time direction will be almost completely decoupled from the dynamics of the rest of the string coordinates, appearing only through the Virasoro conditions. These conditions represent only a selection rule upon the states of the  $O(6)$  sigma model allowing to choose a particular set of states, or a particular set of solutions in the classical limit, which do not contain any dynamics along the string.

Of course in the absence of fermions and the AdS part of the full 10D superstring theory, this model will be asymptotically free and will not be suitable as a viable quantum string theory. In addition, on the dual  $\mathcal{N} = 4$  Yang–Mills side, the corresponding  $\mathfrak{so}(6)$  sector of bosons is not closed under the action of dilatation operator (except the limit of long operators which can be compared with the classical string [69]). However, in the classical limit we will encounter the full classical finite gap solution of the string in  $SO(6)$  sector found in [21]. Furthermore we still expect to capture some features of the full quantum string  $\sigma$ -model.

In the rest of this section we will first take instead of  $O(6)$  a more general  $O(2n)$  case. We will later reproduce the full classical finite gap solution [21] of this model by means of the Zamolodchikovs' physical S-matrix which may be considered as the most convincing demonstration of the correctness of the quantization of the model by the bootstrap method.

### 2.1 Definition of the Sigma-Model on $S^{2n-1}$ and Virasoro Conditions

The  $S^5 \times R_t$  reduction of Green-Schwarz-Metsaev-Tseytlin superstring on  $AdS_5 \times S^5$  background [5, 70] in the orthogonal gauge has a simple action [12] in terms of homogeneous target space coordinates  $X_i(\tau, \sigma)$ ,  $i = 1, \dots, 2n$  and a scalar  $Y(\tau, \sigma)$  representing the AdS time:

$$S = \frac{\sqrt{\lambda}}{4\pi} \int_0^{2\pi} d\sigma \int d\tau [(\partial_a X_i)^2 - (\partial_a Y)^2], \quad X_i X_i = 1. \quad (2.1)$$

The coupling constant in front of the action is identified by the AdS/CFT correspondence with the 't Hooft coupling  $\lambda = g^2 N_c$  of the  $\mathcal{N} = 4$  supersymmetric Yang–Mills (SYM) theory.

We work in the static gauge  $Y(\tau, \sigma) = \kappa\tau$ . The Virasoro condition reads

$$\text{tr}(j_{\pm})^2 = -2(\partial_{\pm} Y)^2 = -2\kappa^2, \quad \partial_{\pm} = \partial_{\tau} \pm \partial_{\sigma} \quad (2.2)$$

where the current is a  $6 \times 6$  matrix defined as

$$(j_{\pm})_{ab} = (h^{-1} \partial_{\pm} h)_{ab} = 2(X_a \partial_{\pm} X_b - \partial_{\pm} X_a X_b), \quad h_{ab} = \delta_{ab} - 2X_a X_b. \quad (2.3)$$

$\Delta = \sqrt{\lambda} \kappa$  is identified with the dimension of the corresponding SYM operator according to the AdS/CFT correspondence.

To illuminate the difference between the string sigma-model on  $S^5 \times R_t$  and the ordinary sigma-model on  $S^5$ , it is instructive to consider slightly more general constraints. These constraints can be viewed as the Virasoro constraints for another gauge

$$Y = \frac{1}{2} \kappa_+ (\tau + \sigma) + \frac{1}{2} \kappa_- (\tau - \sigma). \quad (2.4)$$

AdS time  $Y$  is periodically compactified in this case.

$$\text{tr}(j_{\pm})^2 = -2 \kappa_{\pm}^2. \quad (2.5)$$

The complete Virasoro conditions forbidding the time compactification will be imposed by the identification  $\kappa_+ = \kappa_- = \kappa$ . Note that the condition eq.(2.5) still allows a nonzero longitudinal momentum, although its density, as well as the energy density are constant along the string.

In what follows we will deal with the action

$$S = \frac{\sqrt{\lambda}}{4\pi} \int_0^{2\pi} d\sigma \int d\tau (\partial_a X_i)^2 = -\frac{\sqrt{\lambda}}{32\pi} \int d^2\sigma \text{tr}(j_a j_a), \quad (2.6)$$

subject to the condition eq.(2.5), with an arbitrary number of fields  $X_i$ ,  $i = 1, \dots, 2n$ .

The energy and the momentum are given by

$$E^{\text{cl}} \pm P^{\text{cl}} = -\frac{\sqrt{\lambda}}{32\pi} \int d^2\sigma \text{tr}[j_0 \pm j_1]^2, \quad (2.7)$$

or, using (2.5),

$$E^{\text{cl}} = \frac{\sqrt{\lambda}}{4} (\kappa_+^2 + \kappa_-^2), \quad P^{\text{cl}} = \frac{\sqrt{\lambda}}{4} (\kappa_+^2 - \kappa_-^2). \quad (2.8)$$

## 2.2 Classical Integrability and Finite Gap Solution

The equations of motion and the form of the current,  $j = h^{-1} dh$ , can be encoded into a single flatness condition [67]

$$[\mathcal{L}_+(x), \mathcal{L}_-(x)] = 0, \quad (2.9)$$

where the Lax pair of operators, the currents deformed by spectral parameter  $x$ , are given by

$$\mathcal{L}_{\pm}(x) = \partial_{\pm} - \frac{j_{\pm}}{x \mp 1}. \quad (2.10)$$

The Lax operators describe a connection over the world-sheet and define the monodromy matrix

$$\Omega(x) = \overleftarrow{P} \exp \int_0^{2\pi} d\sigma \frac{1}{2} \left( \frac{j_+}{x-1} + \frac{j_-}{x+1} \right). \quad (2.11)$$

By construction  $\Omega(x)$  is a complex orthogonal matrix and thus has the eigenvalues

$$\left( e^{i\hat{q}_1(x)}, e^{-i\hat{q}_1(x)}, e^{i\hat{q}_2(x)}, e^{-i\hat{q}_2(x)}, \dots, e^{i\hat{q}_n(x)}, e^{-i\hat{q}_n(x)} \right) \quad (2.12)$$



where  $q_k(x)$  are called quasi-momenta. They do not depend on time  $\tau$  due to eq.(2.9) and provide an infinite set of classical integrals of motion of the model. As for the global conserved charges of the sigma-model one has

$$J = \frac{\sqrt{\lambda}}{4\pi i} \int_0^{2\pi} d\sigma j_\tau = \text{diag} (J_1, -J_1, J_2, -J_2, \dots, J_n, -J_n) . \quad (2.13)$$

This current is normalized so that after quantization  $J_i$  are integers for any quantum state. This is the  $O(2n)$  angular momenta quantization condition.

Let us now recall some analytic properties of these quasi-momenta [21]. Expanding the monodromy matrix in powers of  $1/x$  around  $x = \infty$ , we obtain

$$\hat{q}_k(x) = \frac{1}{x} \frac{4\pi J_k}{\sqrt{\lambda}} + \mathcal{O}(1/x^2) . \quad (2.14)$$

We see from (2.11) that simple poles will appear at  $x = \pm 1$  for the quasi-momenta. Furthermore, from (2.3) we see that  $j$  has only 2 eigenvectors corresponding to nonzero eigenvalues. Thus we can diagonalize  $j_\pm$  in such a way that the poles at  $\pm 1$  are only present in  $q_1$ ,

$$\hat{q}_k(x) = \delta_{k,1} \frac{2\pi\kappa_\pm}{x \mp 1} + \mathcal{O}((x \mp 1)^0) \quad \text{for } x \rightarrow \pm 1 . \quad (2.15)$$

Furthermore the monodromy matrix (2.11) with inverse spectral parameter,  $\Omega(1/x)$ , can be written, using the explicit form (2.3) of  $j$  and  $h$ , as

$$\Omega(1/x) = \overleftarrow{P} \exp \int_0^{2\pi} d\sigma \left( h^{-1} \frac{1}{2} \left( \frac{j_+}{x-1} + \frac{j_-}{x+1} \right) h - h^{-1} \partial_\sigma h \right) = h(2\pi) \Omega(x) h^{-1}(0) .$$

which is nothing but a similarity transformation due to the periodicity  $h(2\pi) = h(0)$ . Therefore  $\Omega(x)$  and  $\Omega(1/x)$  have the same set of eigenvalues. For the quasi-momenta this gives the transformation law

$$\hat{q}_k(1/x) = \delta_{k,1} (4\pi m - \hat{q}_1(x)) + (1 - \delta_{k,1}) \hat{q}_k(x) \quad (2.16)$$

which respects (2.15). This symmetry will be of utmost importance in our further discussions. From this relation one immediately reads off the analytic behavior of  $\hat{q}_k$  around  $x = 0$  giving the behavior around  $x = \infty$ .

Finally we obtain the quasi-momentum by solving the characteristic polynomial of  $\Omega$  which is well defined in  $\mathbb{C}$ . This, on the other hand, implies that the quasi-momenta will be the  $2n$  branches of a single function with branch cuts  $\mathcal{C}_a$ . Along these cuts the quasi-momenta in general get permuted and shifted by multiples of  $2\pi$  as

$$\hat{q}_k \mp \hat{q}_l = 2\pi n_a , \quad x \in \mathcal{C}_a , \quad (2.17)$$

so that we obtain some sheets connected by the cuts as in the example in figure 6. For each cut outside the unit circle there will be a mirror cut inside the unit circle due to (2.16).

### 2.3 Classical $SU(2)$ Principal Chiral Field

In this subsection we will concentrate on the classical finite gap solution of the  $O(4)$  sigma model formulated in terms of the  $SU(2)$  principal chiral field. We will essentially briefly repeat the construction of [19] (with a small generalization to the excitations of both left and right sectors) to fix the notations for the easy comparison with the quantum Bethe ansatz solution of the model.

### 2.4 Definition of the Model

The  $O(4)$  sigma model represents the reduction of the sigma model in the  $AdS_5 \times S^5$  background to the subsector of string moving on  $S^3 \times R_t$ . Classically this is a perfectly consistent reduction while at the quantum level one might still expect to capture some features of the full theory. The action of the theory can be represented in terms of the  $SU(2)$  group valued field  $g = X_1 + i\tau_3 X_2 + i\tau_2 X_3 + i\tau_1 X_4$  ( $\tau_i$  are the Pauli matrices). Then the action eq.(2.6) takes the form of the  $SU(2)$  principal chiral field

$$S = \frac{\sqrt{\lambda}}{8\pi} \int_0^{2\pi} d\sigma \int \text{tr}(\partial_a g^\dagger \partial_a g). \quad (2.18)$$

The obvious global symmetry of the action is the left and right multiplication by  $SU(2)$  group element. The currents of this symmetry are

$$j_\pm^R = g^{-1} \partial_\pm g, \quad j_\pm^L = \partial_\pm g g^{-1}, \quad (2.19)$$

with corresponding Noether charges

$$Q_L = \frac{\sqrt{\lambda}}{4\pi} \int d\sigma \text{tr} \left( i \partial_0 g g^\dagger \tau^3 \right), \quad Q_R = \frac{\sqrt{\lambda}}{4\pi} \int d\sigma \text{tr} \left( i g^\dagger \partial_0 g \tau^3 \right). \quad (2.20)$$

In the quantum theory these charges are positive integers. It will be important for future comparisons to notice that the normalization of the generators is such that the smallest possible charge is 1.

Virasoro conditions read

$$\text{tr}(j_\pm^2) = -2 \kappa_\pm^2. \quad (2.21)$$

From the action we read off the energy and momentum as

$$E^{\text{cl}} \pm P^{\text{cl}} = -\frac{\sqrt{\lambda}}{8\pi} \int \text{tr}[j_0 \pm j_1]^2 d\sigma = \frac{\sqrt{\lambda}}{2} \kappa_\pm^2. \quad (2.22)$$

The Lax construction (2.9-2.11) can be repeated for this formulation using either the left or the right current, the two choices being related by a simple relation

$$\Omega_L(1/x) = g(2\pi) \Omega_R(x) g^{-1}(0). \quad (2.23)$$

Let us use  $\Omega_R$ , for definiteness. Now there will be only two quasi-momenta  $p_1(x), p_2(x)$  since the  $2 \times 2$  unitary monodromy matrix  $\Omega(x)$  will have eigenvalues  $e^{ip_1(x)}, e^{ip_2(x)}$ . Unimodularity imposes

$$\tilde{p}_1(x) = -\tilde{p}_2(x) \pmod{2\pi} \quad (2.24)$$

so that we can define

$$T(x) \equiv \frac{1}{2} \text{Tr} \Omega_R(x) \equiv \cos \tilde{p}(x). \quad (2.25)$$

Analyzing the singularities of eq.(2.11) we find the behavior of the quasi-momentum at  $x \rightarrow \infty$

$$\tilde{p}(x) = -\frac{2\pi Q_R}{\sqrt{\lambda} x} + \dots, \quad (2.26)$$

and at  $x \rightarrow 0$  (from eq.(2.23))

$$\tilde{p}(x) \sim 2\pi m + \frac{2\pi Q_L}{\sqrt{\lambda}} x + \dots, \quad (2.27)$$

where we also used the fact that due to the periodicity of  $g(\sigma)$ ,  $\Omega(0) = 1$  and hence  $\tilde{p}(0) = 2\pi m$ . Finally, at  $x \rightarrow \pm 1$

$$\tilde{p}(x) = -\frac{\pi \kappa_{\pm}}{x \mp 1} + \dots, \quad (2.28)$$

By construction  $\Omega_R(x)$  is analytical in the whole plane except  $x = \pm 1$  where one has essential singularities. Then, from eq.(2.25), one concludes that for  $x \neq \pm 1$  the only singularities of

$$\tilde{p}'(x) = -\frac{T'(x)}{\sqrt{1-T^2(x)}} \quad (2.29)$$

can be of the type  $\tilde{p}'(x \rightarrow x_k) \sim \frac{1}{\sqrt{x-x_k}}$ . If we look for the finite gap solution the number of these branch points is finite and even, and we conclude from (2.26-2.29) that the  $\tilde{p}'_1(x), \tilde{p}'_2(x)$  are two branches of an analytical function defined by a hyperelliptic curve of genus  $g$ :

$$[\tilde{p}'(x)]^2 = \left( \frac{b_+}{(x-1)^2} + \frac{b_-}{(x+1)^2} + \frac{c_+}{x-1} + \frac{c_-}{x+1} + P_{g-1}(x) \right)^2 \frac{1}{\prod_{k=1}^{2(g+1)} (x-x_k)} \quad (2.30)$$

The coefficients of the polynomial  $P_{g-1}(x)$  of degree  $g-1$  and  $b_{\pm}, c_{\pm}$ , and the positions of branch points  $x_k$  make a total of  $3g+6$  constants. They are fixed by

1. The asymptotics (2.26-2.28) and the absence of simple poles at  $x = \pm 1$  (5 conditions).
2. The singlevaluedness conditions

$$\oint_{A_j} d\tilde{p} = 0 \quad j = 1, \dots, g \quad (2.31)$$

where the homomorphic integrals around the cycles  $A_i$  are essentially the contour integrals around the cuts  $C_k$  ( $g$  conditions).

3. The integer  $B$ -period conditions, analogous to eq.(2.17)

$$\oint_{B_j} d\tilde{p} = 2\pi n_j \quad j = 1, \dots, g + 1. \quad (2.32)$$

following from the ambiguity of the definition of the branches of the quasi-momentum eq.(2.24) ( $g + 1$  conditions).

The cycle  $A_i$  is the contour which encircles the cut  $C_i$  – see figure 4 – in the counterclockwise direction in the upper sheet if the cut is outside the unit circle or in the clockwise direction in the lower sheet if it is inside the unit circle.

The  $B_k$  cycle consists of the contour starting at  $\infty_+$  in the upper sheet, changing sheet in at the cut  $C_k$  and going from here to  $\infty_-$  in this lower sheet.

We can also write (2.27) as

$$\oint_{B_\theta} d\tilde{p} = 2\pi m. \quad (2.33)$$

where this new cycle goes from  $\infty$  to 0 in the upper sheet.

Let us distinguish the cuts inside and outside the unit circle by superscripts  $u$  and  $v$ . The remaining  $g$  constants can be parametrized by the filling fraction numbers which we define as

$$S_i^v = -\frac{\sqrt{\lambda}}{8\pi^2 i} \oint_{A_i^v} \tilde{p}(x) \left(1 - \frac{1}{x^2}\right) dx, \quad S_i^u = \frac{\sqrt{\lambda}}{8\pi^2 i} \oint_{A_i^u} \tilde{p}(x) \left(1 - \frac{1}{x^2}\right) dx \quad (2.34)$$

From the AdS/CFT correspondence these filling fractions are expected to be integers since this is obvious on the SYM side [19, 24]. In fact, it was pointed out in [21, 24] and shown in [66] that  $S_i^{u,v}$  are action variables so that quasi-classically they indeed become integers. We also find a striking evidence for this quantization in the string side when finding the classics from the quantum Bethe ansatz where these quantities are naturally quantized.

The conditions eq.(2.33) can also be represented as

$$\tilde{p}(x) = 2\pi n_k, \quad x \in C_k \quad (2.35)$$

where we defined

$$\tilde{p}(x) = \frac{1}{2} (\tilde{p}(x + i0) + \tilde{p}(x - i0)). \quad (2.36)$$

### 3 Quantum Bethe Ansatz and Classical Limit: $O(4)$ Sigma-Model

We will describe a quantum state of the  $O(n)$  sigma model (the analogue of the "closed string" state for the  $S^3 \times R_1$  sector of the superstring theory) by a system of  $L$  physical particles of the mass  $m_0$  put on a circle of the length  $\mathcal{L}$ . These particles transform in the vector representation under  $O(4)$  symmetry group or in the bi-fundamental representations of  $SU(2)_R \times SU(2)_L$ . The scattering of the particles in this theory is known to be elastic and factorizable: the relativistic S-matrix  $\hat{S}(\theta_1 - \theta_2)$  depends only on the difference of rapidities of scattering particles  $\theta_1$  and  $\theta_2$  and obeys the Yang–Baxter equations. As was shown in [38] (and in [40, 41, 43, 44] for the general

principle chiral field) these properties, together with the unitarity and crossing-invariance, define essentially unambiguously the S-matrix. In Appendix C we review the Bootstrap program of [38] as well and the algebraic Bethe ansatz construction for this system [71].

There should be no confusion with the employed notation. Having in mind the comparison in section 4 we will use the same letters in sections 2 and 3 for quantities that we be later proven to be the same. For what concerns this section they are just definitions.

### 3.1 Bethe Equations for Particles on a Circle

When this system of particles is put into a finite 1-dimensional periodic box of the length  $\mathcal{L}$  the set of rapidities of the particles  $\{\theta_\alpha\}$  is constrained by the condition of periodicity of the wave function  $|\psi\rangle$  of the system,

$$|\psi\rangle = e^{i\mu \sinh \pi \theta_\alpha} \prod_1^{\overleftarrow{\alpha-1}} \hat{S}(\theta_\alpha - \theta_\beta) \prod_N^{\overrightarrow{\alpha+1}} \hat{S}(\theta_\alpha - \theta_\beta) |\psi\rangle \quad (3.1)$$

where the first term is due to the free phase of the particle and the second is the product of the scattering phases with the other particles. Arrows stand for ordering of the terms in the product.  $\mu = m_0 \mathcal{L}$  is a dimensionless parameter. The physical  $SU(2)$  PCF S-matrix is a product of left and right S-matrices,  $\hat{S} = \hat{S}_L \times \hat{S}_R$  [38, 40]

$$\hat{S}_{L,R}(\theta) = S_0(\theta) \left( P_{L,R}^+ + \frac{\theta + i}{\theta - i} P_{L,R}^- \right) \quad \text{or} \quad \left( \hat{S}_{R,L}(\theta) \right)_{ab}^{a'b'} = \frac{S_0(\theta)}{\theta - i} \left( \theta \delta_a^{a'} \delta_b^{b'} - i \delta_a^{b'} \delta_b^{a'} \right)$$

and

$$S_0(\theta) = i \frac{\Gamma(-\frac{\theta}{2i}) \Gamma(\frac{1}{2} + \frac{\theta}{2i})}{\Gamma(\frac{\theta}{2i}) \Gamma(\frac{1}{2} - \frac{\theta}{2i})}, \quad (3.2)$$

It has the following large  $\theta$  asymptotics:

$$i \log S_0^2(\theta) \sim 1/\theta + O(1/\theta^3). \quad (3.3)$$

The diagonalization of both the L and R factors in the process of fixing the correct periodicity (3.1) leads to the following set of Bethe equations

$$e^{-i\mu \sinh \pi \theta_\alpha} = \prod_{\beta \neq \alpha} S_0^2(\theta_\alpha - \theta_\beta) \prod_j \frac{\theta_\alpha - u_j + i/2}{\theta_\alpha - u_j - i/2} \prod_k \frac{\theta_\alpha - v_k + i/2}{\theta_\alpha - v_k - i/2}, \quad (3.4)$$

$$1 = \prod_\beta \frac{u_j - \theta_\beta - i/2}{u_j - \theta_\beta + i/2} \prod_{i \neq j} \frac{u_j - u_i + i}{u_j - u_i - i}, \quad (3.5)$$

$$1 = \prod_\beta \frac{v_k - \theta_\beta - i/2}{v_k - \theta_\beta + i/2} \prod_{l \neq k} \frac{v_k - v_l + i}{v_k - v_l - i}, \quad (3.6)$$

where

$$\alpha, \beta = 1, \dots, L, \quad i, j = 1, \dots, J_u, \quad k, l = 1, \dots, J_v.$$

The left and right charges of the Bethe vector, i.e. wave function, associated with the two  $SU(2)$  spins are given by

$$Q_L = L - 2J_u, \quad Q_R = L - 2J_v, \quad (3.7)$$

since a  $u$  or  $v$  root correspond to a spin flip in the corresponding  $SU(2)$  and since we are normalizing charges so that 1 is the unit charge. The absence of  $u$ 's and  $v$ 's corresponds to the ferromagnetic limit with all spins aligned in the up direction.

Both the construction of the  $S$ -matrix by means of the bootstrap program [38] and these Bethe equations (see a similar example in [71]) describing the solution to (3.1) are reviewed in Appendix C for the sake of completeness.

The total momentum and the total energy of the state are the sums of momenta and energies of individual particles. In accordance with eq.(2.18) we take  $\mathcal{L} = 2\pi$  (in the units of the string tension). Then

$$P = \frac{\mu}{2\pi} \sum \sinh(\pi\theta_\alpha), \quad (3.8)$$

$$E = \frac{\mu}{2\pi} \sum \cosh(\pi\theta_\alpha) \quad (3.9)$$

This model with massive relativistic particles and the asymptotically free UV behavior cannot look like a consistent quantum string theory. Only in the classical limit we can view it as a string toy model obeying the classical conformal symmetry. In the classical case it is also easy to impose the Virasoro conditions eq.(2.5). In quantum case, we still can try to impose the Virasoro conditions, but they will be already some conditions selecting the quantum states. It is not easy on the stage of Bethe equations, but we will later make some plausible conjecture concerning this selection.

### 3.2 The Classical Limit

In the classical limit,  $\mu = \mathcal{L}m_0 \rightarrow 0$ , the physical mass of the particle  $m_0 \sim \mathcal{L}^{-1}e^{-\sqrt{\lambda}/2}$  is small in the units of inverse length  $\mathcal{L}^{-1}$  of the circle on which we put a large number  $L \rightarrow \infty$  of particles, keeping  $J_u \sim J_v \sim L$  as well. In this limit the Bethe roots  $u_k, v_k, \theta_k$  (and the characteristic distances between them) are large, of the order of  $L$ . So we can take  $\log$ 's of Bethe equations eq.(3.1) and use the "Coulomb" approximation eq.(3.3) for  $S_0(\theta)$ , as well as for other terms:  $\log \frac{u+i/2}{u-i/2} = \frac{i}{u} + O(1/u^3)$ .<sup>7</sup> Therefore it is useful to rescale

$$u = Mx, \quad v = My, \quad \theta = M\xi$$

---

<sup>7</sup>This limit, sometimes called thermodynamical (which is a bit misleading since the energy is not proportional to the length of the system) in the context of ferromagnetic spin chains was suggested in [16] and considerably advances in papers [17,18]; see also [24] where an important phenomenon of the anomaly cancelation was observed, vital for the validity of this limit. The antisymmetry of the  $\log$ 's of all factors in (3.4-3.6), including  $\log S(\theta)$ , is also important for the validity of the approximation.

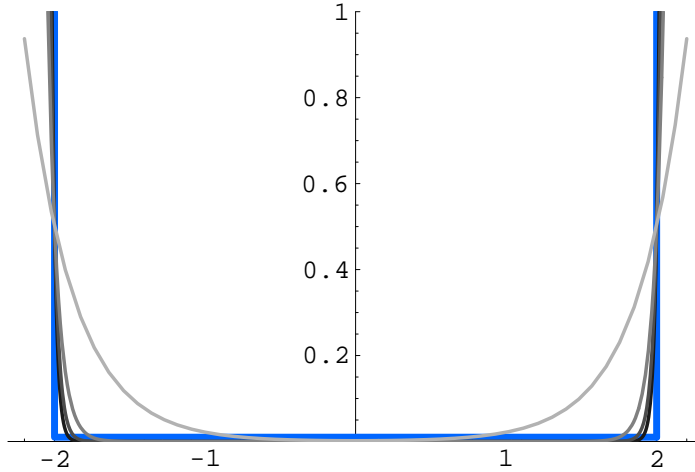


Figure 1: We plot  $V(\xi)$  for  $M = 1, 5, 9, 13$  (lighter to darker gray). It is clear that the potential approaches the blue box potential as  $M \rightarrow \infty$ .

where we chose

$$M \equiv -\frac{\log \mu}{2\pi} \sim L.$$

Taking log of each Bethe equation (3.4-3.6) we arrive at the following system of equations

$$\mu \sinh \pi M \xi_\alpha = \frac{1}{M} \sum_{\beta \neq \alpha} \frac{1}{\xi_\alpha - \xi_\beta} - \frac{1}{M} \sum_j \frac{1}{\xi_\alpha - x_j} - \frac{1}{M} \sum_k \frac{1}{\xi_\alpha - y_k} + 2\pi m_\alpha, \quad (3.10)$$

$$0 = -\frac{1}{M} \sum_\beta \frac{1}{x_j - \xi_\beta} + \frac{2}{M} \sum_{i \neq j} \frac{1}{x_j - x_i} - 2\pi n_j^u, \quad (3.11)$$

$$0 = -\frac{1}{M} \sum_\beta \frac{1}{y_k - \xi_\beta} + \frac{2}{M} \sum_{l \neq k} \frac{1}{y_k - y_l} - 2\pi n_k^v, \quad (3.12)$$

where  $m_\alpha, n_j^u, n_k^v$  are integers corresponding to the choice of a branch of logarithm. We will call them mode numbers since they are the analogue of the mode numbers of oscillators in the string theory.

It reminds a system of 2D Coulomb charges of different species in static equilibrium, each one in its own constant field of force  $2\pi m_\alpha, 2\pi n_j^u, 2\pi n_k^v$ , respectively, and in a confining potential for  $\theta$ 's

$$V(\xi) = \mu \cosh(\pi M \xi). \quad (3.13)$$

In our limit  $M \sim \log \mu^{-1} \rightarrow \infty$ , the potential for  $\xi \sim 1$  basically looks as a box with almost vertical walls (the “thickness” of the wall is of the order  $1/M$ ) - see figure 1. The positions of the walls  $\xi = \pm t$  defining the width of distribution of  $\theta$ 's can be estimated with the logarithmic accuracy from  $V(t) \simeq 1$ . One has therefore

$$t = \frac{1}{\pi M} (\log \mu^{-1} + \mathcal{O}(M^0)) \simeq 2.$$

All this tells us that we can write the continuum version of Bethe equations, similarly to the large  $N$  limit of matrix models, in terms of the resolvents of root distributions:

$$G_\theta(x) \equiv \frac{1}{M} \sum_{\beta=1}^L \frac{1}{z - \xi_\beta}, \quad G_u(z) \equiv \frac{1}{M} \sum_{i=1}^{J_u} \frac{1}{z - x_i}, \quad G_v(z) \equiv \frac{1}{M} \sum_{l=1}^{J_v} \frac{1}{z - y_l}.$$

with the large  $z$  asymptotics

$$G_u(z) \simeq \frac{J_u}{M} \frac{1}{z}, \quad G_v(z) \simeq \frac{J_v}{M} \frac{1}{z}, \quad G_\theta(z) \simeq \frac{L}{M} \frac{1}{z}. \quad (3.14)$$

These equations are defined on the distribution supports  $\mathcal{C}_u, \mathcal{C}_\theta, \mathcal{C}_v$ , each characterized by the corresponding integer mode number  $n_u, n_v$  or  $m$ :

$$\begin{aligned} 2\mathcal{G}'_u(z) - G_\theta(z) &= 2\pi n_u, & z \in \mathcal{C}_u \\ \mathcal{G}'_\theta(z) - G_v(z) - G_u(z) &= -2\pi m, & z \in \mathcal{C}_\theta \\ 2\mathcal{G}'_v(z) - G_\theta(z) &= 2\pi n_v, & z \in \mathcal{C}_v \end{aligned} \quad (3.15)$$

There can be as many cuts as there are different mode numbers. Note that we dropped the potential term for  $\xi$ 's in the second eq. since, as we explained, it is zero within the infinite walls at  $\xi = \pm 2$ . The only trace left by the potential, as shown in Appendix A, is the behavior of  $G_\theta(z) \sim \frac{1}{\sqrt{z \pm 2}}$  near the walls of the box which we should impose on the solutions of eq.(3.15).

Equation (3.15) can also be written in terms of densities defined by

$$\rho_\theta(x) = \lim_{M \rightarrow \infty} \frac{1}{M} \sum_{\alpha} \delta(z - \xi_\alpha),$$

and similar for  $u$ 's and  $v$ 's. Then, for example, second line in eq.(3.15) becomes

$$\int_{\mathcal{C}_\theta} \frac{\rho_\theta(w)}{z - w} dw - \int_{\mathcal{C}_u} \frac{\rho_u(w)}{z - w} dw - \int_{\mathcal{C}_v} \frac{\rho_v(w)}{z - w} dw = -2\pi m, \quad z \in \mathcal{C}_\theta. \quad (3.16)$$

We considered only one mode number  $m$ . Later it will be shown that in order to reproduce the finite gap solutions for classical strings on  $S^3 \times R_t$  we have to assume that we have a single cut  $[-2, 2]$  for  $\xi$ -distribution characterized with all Bethe roots  $\theta_k$ ,  $k = 1, \dots, L$  having the same mode number  $m$ . As we will argue in section 5.2 the *classical* multi-cut states with more mode numbers excited correspond to the longitudinal oscillations of the string. In the string theory these oscillations are non-physical and forbidden by the Virasoro constraints, but they are present in the standard relativistic  $\sigma$ -model eq.(2.18). We know how to do it in the classical limit, but it is more difficult to project it in the full quantum space of states. It is also plausible to assume that not only in the classical, but also in full quantum theory, *only the Bethe states with  $\theta_\alpha$ ,  $\alpha = 1, \dots, L$ , having the same mode number  $m$  obey the Virasoro constraints*. We don't have for the moment any convincing proof of this conjecture, apart from some examples and the comparison of the classical limit of our Bethe equations with the classical finite gap solution of section 4.



The total momentum can be calculated exactly, before any classical limit

$$P = \frac{\mu}{2\pi} \sum_{\alpha} \sinh(\pi\theta_{\alpha}) = mL - \sum_p n_p S_p^u - \sum_p n_p S_p^v \quad (3.17)$$

where  $S_p^u, S_p^v$  are the filling fractions, or the numbers of Bethe roots with a given mode numbers  $n_{u,p}, n_{v,p}$ . To prove it it suffices to take the sum of logarithms of the eq.(3.4) for all roots  $\theta_{\alpha}$ . The contribution of  $S_0(\theta)$  terms cancels due to antisymmetry while the second and third sums in the r.h.s. of (3.10) are excluded using (3.5) and (3.6) respectively.

For the closed string theory we should take  $P = 0$ , which gives the level matching condition. For the perturbative super YM applications one should take  $S_p^u = 0$  [69]. Then we have the well known formula  $\sum_p n_p S_p^v = mL$  (see [19] for details).

Let us now study the system of equations eq.(3.15) as a Riemann-Hilbert problem, first for the highest weight states with  $U(1)$  symmetry, without magnon excitations  $u_k$  and  $v_k$ , and than for a general classical state. Our goal will be to reproduce (and to generalize from a single sector to both left and right sectors) the finite gap results and the corresponding algebraic curve of the paper [19].

### 3.3 Highest Weight States of $U(1)$ Sector in Classical Limit

If the right and left modes are not excited we have only the states with  $U(1)$  modes, which means that the currents  $j_L = j_R$  are diagonal matrices.

In the classical limit, using the Coulomb approximation, we have for this sector the following Bethe equation

$$\mu \sinh \pi M \xi_{\alpha} - 2\pi m = -\frac{1}{M} \sum_{\beta \neq \alpha}^L \frac{1}{\xi_{\alpha} - \xi_{\beta}}.$$

In the continuous limit, the equation for the asymptotic density,  $L \sim M \rightarrow \infty$ , is given by

$$\mathcal{G}_{\theta}(x) = -2\pi m, \quad x \in \mathcal{C}_{\theta}, \quad (3.18)$$

with inverse square root boundary conditions near  $\pm 2$  (see Appendix A and discussion in previous subsection). The asymptotic density of rapidities,  $\rho_{\theta}(z)$ , is obtained through the resolvent from

$$\rho_{\theta}(z) = -\frac{1}{2\pi i} (G_{\theta}(z+i0) - G_{\theta}(z-i0)).$$

The analytical function  $G_{\theta}(x)$  having a real part on the cut defined by eq.(3.18), with support  $[-2, 2]$ , with inverse square root boundary conditions and behaving at  $z \rightarrow \infty$  as  $G_{\theta}(z) \rightarrow \frac{L}{M} \frac{1}{z}$  is completely fixed:

$$G_{\theta}(z) = \left( \frac{2\pi m z + \frac{L}{M}}{\sqrt{z^2 - 4}} - 2\pi m \right) \quad (3.19)$$

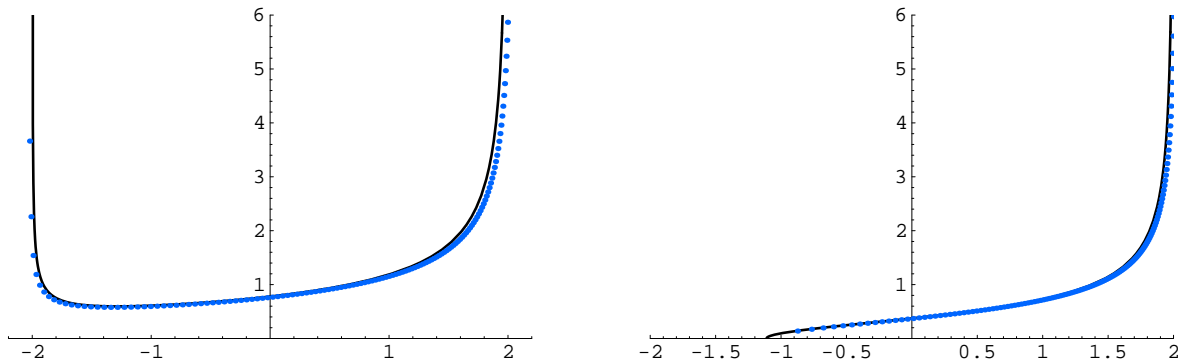


Figure 2: Density of  $\theta$ -roots before and after phase transition. Black line - asymptotic densities of eqs.(3.20,3.28), blue dots - numerical solution for  $L = 150$  roots.

which gives for the density

$$\rho_{\theta}(z) = \frac{1}{\pi} \left( \frac{2\pi m z + \frac{L}{M}}{\sqrt{4 - z^2}} \right). \quad (3.20)$$

Notice that the distribution has a singular behavior at the endpoints which will be the typical behavior even for the general multi-cut solution which we study in the next subsection. Notice also that applying to the eq.(3.19) the Zhukovsky map

$$z = x + \frac{1}{x} \quad (3.21)$$

we obtain

$$G_{\theta}(z(x)) = \frac{\frac{L}{2M} + 2\pi m}{x - 1} + \frac{\frac{L}{2M} - 2\pi m}{x + 1} \quad (3.22)$$

which shows the poles at  $x = \pm 1$ , typical for the finite gap solution of the section 1. The Zhukovsky map will be the central piece of our proof of the identification of the continuous limit of Bethe ansatz equations with general classical solutions of  $\sigma$ -models considered in this paper.

From the general formula eq.(3.17) the momentum of such a state is

$$P = mL \quad (3.23)$$

Let us now compute the energy of this state in the continuous limit (it is derived in greater detail in Section 3.5 for a general state). We have to compute the sum

$$E \equiv \frac{\mu}{2\pi} \sum_{\alpha} \cosh(\pi M \xi_{\alpha}) \simeq \sum_{\xi_{\alpha} > 0} \frac{\mu}{\pi} \sinh(\pi \xi_{\alpha} M) - \sum_{\xi_{\alpha} < 0} \frac{\mu}{\pi} \sinh(\pi \xi_{\alpha} M)$$

where the last equality holds with exponential precision since the decaying exponents of the *sinh*'s can be dropped. Then, by the use of Bethe ansatz equations for each of the *sinh*'s we get

$$E \simeq \frac{i}{\pi} \sum_{\substack{\xi_{\beta} < 0 < \xi_{\alpha}}} \log S_0^2(M [\xi_{\alpha} - \xi_{\beta}]) + \sum_{\alpha} m \operatorname{sign}(\xi_{\alpha}).$$

Now we do not have a problem, as in eq.(3.24), with badly defined sums of small exponentials. In the scaling limit these sums become integrals

$$E \simeq -\frac{M}{\pi} \int_{-2}^0 dz \int_0^2 dw \frac{\rho_\theta(z)\rho_\theta(w)}{z-w} + m M \int \rho_\theta(z) \text{sign}(z) dz \quad (3.24)$$

where  $\rho_\theta(z)$  is given by eq.(3.20). In fact these integrals can be easily calculated and the result reads

$$E = \frac{L^2}{4\pi M} + 4\pi M m^2. \quad (3.25)$$

This calculation is generalized to an arbitrary solution of eq.(3.4)-(3.6) including the left and right excitations (with arbitrary  $u_k$ 's and  $v_k$ 's) in Section 3.5.

Now notice that if we start *decreasing* the number of particles  $L$ , at the point

$$L^* = 4\pi|m|M \quad (3.26)$$

the density (3.20) will vanish at one of the walls. This point certainly signifies a phase transition in the effective spin chain and a non-analytical change in the classical state. If we continue to decrease  $L$  past this point the new support will now stretch only on the interval  $[-a, 2]$  (for  $m \geq 0$ ) and the distribution in the limit  $z \rightarrow -a$  becomes less singular:  $\rho_\theta(z) \sim \sqrt{a+z}$ . The resolvent satisfying the right behavior at infinity is:

$$G_\theta(z) = 2\pi m \left( \frac{\sqrt{z-2 + \frac{L}{\pi m M}}}{\sqrt{z-2}} - 1 \right) \quad (3.27)$$

which gives for the density

$$\rho_\theta(z) = 2m \sqrt{\frac{z+a}{2-z}} \quad (3.28)$$

where  $a = -2 + \frac{L}{\pi m M}$ . The phase transition corresponds to  $a = 2$ . This phase transition fits nicely with the electrostatic picture point of view since  $m$  plays the role of an electric field which pushes the particles against one of the walls. It is also interesting to note that  $\kappa_+$  and  $\kappa_-$  become of the opposite signs, which, according to 2.4, means that the coordinate  $Y$  becomes space like on the world sheet.

Only  $L > L^*$  looks compatible with the description of the classical finite gap solution of section 2 for the  $SU(2)_L \times SU(2)_R$  sigma model. Only in that case the poles in  $x$  plane will be on the right place at  $x = \pm 1$ . For the string theory the total momentum should be zero  $P = 2\pi m = 0$ , hence the classical limit works well, at least in this highest weight sector. In the presence of L,R-excitations with non-trivial  $u_i, v_i$  roots the phase transition is still possible. It would be very interesting to understand what are the states beyond this phase transition and what classical solutions correspond to such states if any.

### 3.4 General Classical States and Its Algebraic Curve

Let us now reproduce the general classical states in terms of an algebraic curve as a solution of the Bethe ansatz equations (3.15) in the scaling limit.

We define the quasi-momenta by the formulas

$$\begin{aligned} p_1 = -p_2 &= G_u - \frac{1}{2}G_\theta \\ p_3 = -p_4 &= G_v - \frac{1}{2}G_\theta. \end{aligned} \quad (3.29)$$

Then the functions  $p'_1(z), p'_2(z)$  have the cuts of the type  $C_u, C_\theta$ , and  $p'_3(z), p'_4(z)$  have the cuts of the type  $C_v, C_\theta$ . As in the previous section, we consider only the situation with a single cut  $C_\theta$  and any number of  $C_u, C_v$  cuts. We notice that the quasi-momenta  $p'_1(z), p'_2(z), p'_3(z), p'_4(z)$  form four sheets of the Riemann surface of an analytical function  $p'(z)$  (see fig.3). Indeed

$$\begin{aligned} x \in C_u, \quad p_1'^+ - p_2'^- &= 2\mathcal{G}'_u - G'_\theta = 0, \\ x \in C_\theta, \quad p_2'^+ - p_3'^- &= -G'_u - G'_v + \mathcal{G}'_\theta = 0, \\ x \in C_v, \quad p_3'^+ - p_4'^- &= 2\mathcal{G}'_v - G'_\theta = 0, \\ x \in C_\theta, \quad p_4'^+ - p_1'^- &= -G'_u - G'_v + \mathcal{G}'_\theta = 0, \end{aligned}$$

Integrating these equations we restore the mode numbers  $n_u, n_v$  and  $m$ ,

$$\begin{aligned} x \in C_u, \quad p_1^+ - p_2^- &= 2\pi n_u \\ x \in C_\theta, \quad p_2^+ - p_3^- &= 2\pi m \\ x \in C_v, \quad p_3^+ - p_4^- &= 2\pi n_v \\ x \in C_\theta, \quad p_4^+ - p_1^- &= 2\pi m \end{aligned} \quad (3.30)$$

These equations can also be written as holomorphic integrals around the infinite B-cycles:

$$\begin{aligned} \oint_{B_j^u} dp &= 2\pi n_{u,j} \quad n_j = 1, \dots, K_u \\ \oint_{B_j^v} dp &= 2\pi n_{v,j} \quad n_j = 1, \dots, K_v \\ \oint_{B^\theta} dp &= 2\pi m \end{aligned} \quad (3.31)$$

where the the first two conditions correspond to the equations in the first and third line of (3.30), respectively, while the last one corresponds to any of the equations of the second and fourth lines of (3.30). The  $B$  cycles are defined as in fig.3.

From (3.14,3.7) we have the following large  $z \rightarrow \infty$  asymptotics of quasi-momenta on different sheets

$$\begin{aligned} p_1(z) &\simeq -\frac{Q_L}{2M} \frac{1}{z}, & p_2(z) &\simeq \frac{Q_L}{2M} \frac{1}{z}, \\ p_3(z) &\simeq -\frac{Q_R}{2M} \frac{1}{z}, & p_4(z) &\simeq \frac{Q_R}{2M} \frac{1}{z}, \end{aligned} \quad (3.32)$$

The filling fractions, or the numbers of Bethe  $u, v$ -roots forming each cut, are defined as follows:

$$S_i^v = \frac{M}{2\pi i} \oint_{A_i^v} p(z) dz, \quad S_i^u = \frac{M}{2\pi i} \oint_{A_i^u} p(z) dz \quad (3.33)$$

These contours are represented in figure 3.

### 3.5 Energy and Momentum

In this section we will show that the constants  $\kappa_{\pm}$  defined as the square root singularities of the quasi-momenta

$$p_{1,3}(z) = \mp \frac{\pi \kappa_{\pm}}{\sqrt{\pm z - 2}}, \quad |z| > 2 \quad (3.34)$$

are completely fixed by the energy and momentum. At this point we know that (3.17)

$$P = \frac{\mu}{2\pi} \sum_{\alpha} \sinh(\pi \theta_{\alpha}) = mL - \sum_p n_p S_p^u - \sum_p n_p S_p^v. \quad (3.35)$$

Let us now calculate the energy  $E$ . As a byproduct we will also compute the momentum in terms of the singularities at  $z = \pm 2$  described by  $\kappa_{\pm}$ .

We want to compute the sum

$$E \equiv \frac{\mu}{2\pi} \sum_{\alpha} \cosh(\pi \theta_{\alpha}),$$

but we *cannot* simply replace this sum by an integral and use the asymptotic density for  $\theta$ 's to compute the energy. This is because the main contribution for the energy comes from large  $\theta$ 's, near the walls, where the expression for the asymptotic density is no longer accurate. It is natural for the classical limit since the particles become effectively massless, the contributions of right and left modes is clearly distinguishable and are located far from  $\theta = 0$ .

The calculation (3.35) of momentum was simple because we had to sum over  $\sinh \pi \theta_{\alpha}$  which can be taken from the Bethe equations

$$\mu \sinh \pi \theta_{\alpha} = i \sum_{\beta \neq \alpha} \log S_0^2(\theta_{\alpha} - \theta_{\beta}) - \sum_j \frac{1}{\theta_{\alpha} - u_j} - \sum_l \frac{1}{\theta_{\alpha} - v_l} + 2\pi m. \quad (3.36)$$

Now we have to sum over  $\cosh \pi \theta_{\alpha}$ . We notice that the energy is dominated by large  $\theta$ 's where, with exponential precision, we can replace  $\cosh \pi \theta_{\alpha}$  by  $\pm \sinh \pi \theta_{\alpha}$  for positive (negative)  $\theta_{\alpha}$ . Furthermore the contribution from the  $\theta$ 's in the middle of the box is also exponentially suppressed since  $\mu$  is very small. Thus we can pick a point  $a$  somewhere in the box not too close to the walls. One can think of  $a$  as being somewhere in the middle. Then,

$$E = \sum_{\xi_{\alpha} > a} \frac{\mu}{\pi} \sinh(\pi \xi_{\alpha} M) - \sum_{\xi_{\alpha} < a} \frac{\mu}{\pi} \sinh(\pi \xi_{\alpha} M),$$

where, let us stress, the result is *correct and independent of the point  $a$  with exponential precision*. Having a sum of  $\sinh \pi \theta_\alpha$  we can substitute each of them by the corresponding Bethe equation (3.36) obtaining

$$E \simeq \frac{i}{\pi} \sum_{\substack{j,\alpha \\ \xi_\beta < a < \xi_\alpha}} \log S_0^2(M[\xi_\alpha - \xi_\beta]) - \sum_{j,\alpha} \frac{\text{sign}(\xi_\alpha - a)}{\pi(\xi_\alpha - x_j)M} - \sum_{l,\alpha} \frac{\text{sign}(\xi_\alpha - a)}{\pi(\xi_\alpha - y_l)M} + \sum_\alpha m \text{sign}(\xi_\alpha - a).$$

Now we can safely go to the continuous limit since in the first term the distances between  $\xi$ 's are now mostly of order the 1. Moreover, it is very important that the contribution from the  $\xi$ 's near the walls  $\pm 2$  is now suppressed since

$$|\log S_0^2(M(2 - \xi_\beta))| > |\log S_0^2(M(2 - a))| \sim 1/M.$$

This allows to rewrite the energy, with  $1/M$  precision, as follows

$$\begin{aligned} E \simeq & -\frac{M}{\pi} \int_{-2}^a dz \int_a^2 dw \frac{\rho_\theta(z)\rho_\theta(w)}{z-w} - \frac{M}{2\pi} \int \frac{\rho_\theta(z)\rho_u(w)}{z-w} \text{sign}(z-a) dz dw \\ & - \frac{M}{2\pi} \int \frac{\rho_\theta(z)\rho_v(w)}{z-w} \text{sign}(z-a) dz dw + m M \int \rho_\theta(z) \text{sign}(z-a) dz \end{aligned} \quad (3.37)$$

where *the densities are the asymptotic densities for the exact box potential*, given by the integral eq.(3.16).

As a result, by the use of Bethe equations, we managed to transform the original sum over cosh, highly peaked at the walls, into a much smoother sum where the main contribution is now softly distributed along the bulk and where the continuous limit does not look suspicious.

Let us now take (3.37) as our starting point. From the previous discussion we know that this expression does not depend on  $a$  provided  $a$  is not too close to the walls. In fact, we can easily see that it does not depend on  $a$  *at all* after taking the continuous limit leading to the perfect box-like potential. To see this one can see that, due to Bethe equations eq.(3.16), the  $a$ -derivative of this expression is zero for all  $a \in ]-2, 2[$ . Hence we can even send  $a$  close to the wall:  $a = -2 + \epsilon$ , where  $\epsilon$  is very small. Let us calculate the first term. The main contribution to the integral comes from  $-2 \simeq z \sim w$  so that we can use the asymptotics (3.34) to get

$$-\frac{M}{\pi} \int_{-2}^{-2+\epsilon} dz \int_{-2+\epsilon}^2 dw \frac{\rho_\theta(z)\rho_\theta(w)}{z-w} \simeq - \int_{-2}^{-2+\epsilon} dz \int_{-2+\epsilon}^2 dw \frac{4M\kappa_-^2}{\pi(z-w)\sqrt{2+z}\sqrt{2+w}} \simeq 2\pi M\kappa_-^2$$

The remaining 3 terms are very simple: since  $a \simeq -2$  we can simply drop the *sign*-functions inside the integrals and obtain exactly the expression of the momentum in the continuous limit. We arrive therefore at

$$E \simeq 2M\kappa_-^2\pi + \left( mL - \sum_p n_p^v S_p^v - \sum_p n_p^u S_p^u \right). \quad (3.38)$$

where the expression in the parentheses is the momentum. If we compute the  $a$ -independent integral (3.37) near the other wall, i.e. for  $a = 2 - \epsilon$ , we find

$$E \simeq 2M\kappa_+^2\pi - \left( mL - \sum_p n_p^v S_p^v - \sum_p n_p^u S_p^u \right).$$

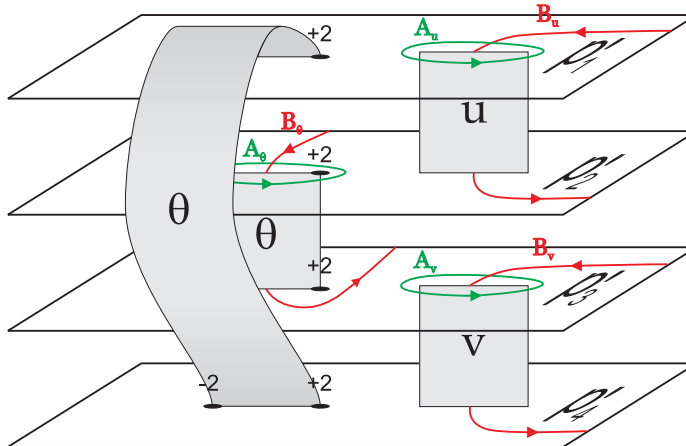


Figure 3: Structure of the curve coming from the Bethe ansatz side. The quasi momenta  $p_{1,2,3,4}(z)$  are defined in (3.29). This figure is related with fig.4 by means of Zhukovsky map.

Therefore, equating the results one obtains the desired expressions for the energy and momentum

$$E \pm P = 2\pi M \kappa_{\pm}^2 \quad (3.39)$$

through the data  $\kappa_{\pm}$  at the singularities of the curve at  $z = \pm 2$ .

#### 4 Matching with the Finite Gap KMMZ Solution

In this section we will demonstrate the main result of our paper: the equivalence of the large density limit of a system of physical particles on a circle for the quantum  $O(4)$   $\sigma$ -model described in the previous section, to the classical theory of the same model described in section 2. On the one hand we have the quantization of the sigma model given by a set of Bethe equations. For this quantum system Virasoro constraints are somewhat obscure. We introduce however a natural selection rule for the quantum states, such that in the scaling limit we obtain the classical finite gap KMMZ solutions for the  $S^3 \times R_t$  classical sigma model with classical Virasoro constraints imposed [19]. Let us also recall that this sector belongs to the superstring theory on  $AdS_5 \times S^5$  and is in itself a consistent classical truncation.

Our result also means that the considered scaling limit of the quantum  $O(4)$   $\sigma$ -model is nothing but the classical limit and our result gives a decisive demonstration of the correctness of Zamolodchikovs' physical bootstrap S-matrix approach [38] to these models, as well as of the Polyakov–Wiegmann solution of the principle chiral field [39]<sup>8</sup>. According to our results, both approaches construct indeed the quantization procedure with the correct classical limit.<sup>9</sup>

More precisely, we will show here that every solution of Bethe ansatz equations in the scaling limit, described by an algebraic curve of the quasi-momentum (3.4-3.6), is in fact a

<sup>8</sup>Although we demonstrate it here only for the  $SU(2)$  case we see no obstacles for the generalization of our method to any  $SU(N)$  principle chiral field.

<sup>9</sup>Modulo the phase transition noticed in the previous section, to the states which are hard to identify with the classical solutions of the underlying classical model.

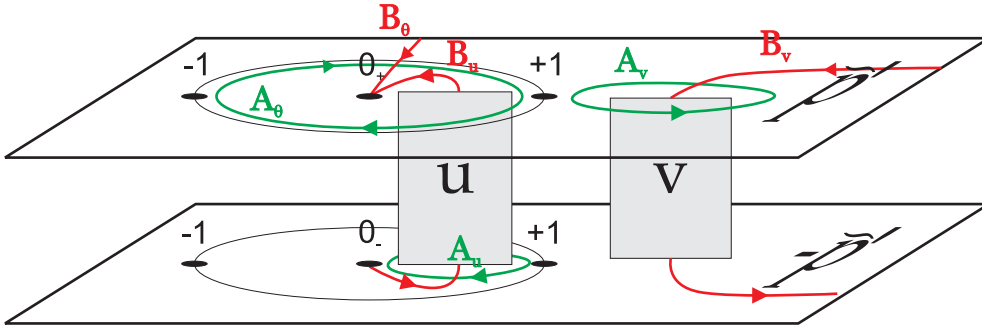


Figure 4: Algebraic curve from the Finite gap method of KMMZ. In this language,  $u$  and  $v$  cuts correspond to cuts inside and outside the unit circle respectively. This figure is related with fig.3 by means of Zhukovsky map.

finite gap solution for the classical string on  $S^3 \times R_t$ . In the next section this correspondence will be generalized to the  $O(6)$  sigma model corresponding to the whole  $S^5 \times R_t$  sector of the classical superstring. The generalization to all  $O(2n)$  sigma models is also straightforward (the corresponding classical string, unlike the quantum one, is well defined).

To prove this correspondence, we have just to compare the algebraic curves describing a Bethe state in the scaling limit and the finite gap curve eq.(2.30), together with all their moduli and the data at singularities. The similar goal for the  $OSP(m + 2n|m)$  model was achieved in [64] by the direct solution of integral Bethe equations.

Central to this comparison will be the Zhukovsky map  $z = x + 1/x$ . We will show that the Riemann surface in  $z$  variable of the scaled Bethe equations, fig.3, on the one hand, and the Riemann surface in  $x$  variable of the classical finite gap solution eq.(2.30), fig.4, on the other hand, are two different projections of the same algebraic curve related by Zhukovsky map. We attempted to present schematically two different projections by different colors of projected parts of the curve fig.5.

When we apply Zhukovsky map to the Riemann surface of fig.3 the  $\theta$ -cuts along  $(-2, 2)$  disappear on all 4 sheets and these singular branch points become simple poles, since under the map

$$\frac{1}{\sqrt{z \pm 2}} \longleftrightarrow \frac{1}{x \pm 1}. \quad (4.1)$$

The Riemann surface in the  $x$  projection will consist only of two sheets, as on fig.4. All the  $u$ -cuts and  $v$ -cuts connect now these two sheets.

The inverse map

$$x_{\pm} = \frac{1}{2} \left( z \pm \sqrt{z^2 - 4} \right) \quad (4.2)$$

projects the two upper sheets of fig.3 with  $u$ -cuts into the interior of the unite circle in  $x$  projection, by means of  $x_-(z)$ , where as the two lower cuts of fig.3 with  $v$ -sheets are projected into the exterior of this unit circle on  $x$  projection, by means of  $x_+(z)$ . More precisely, we will show that

$$p_3(z) = \tilde{p}(x_+(z)), \quad p_1(z) = 2\pi m - \tilde{p}(x_-(z)). \quad (4.3)$$



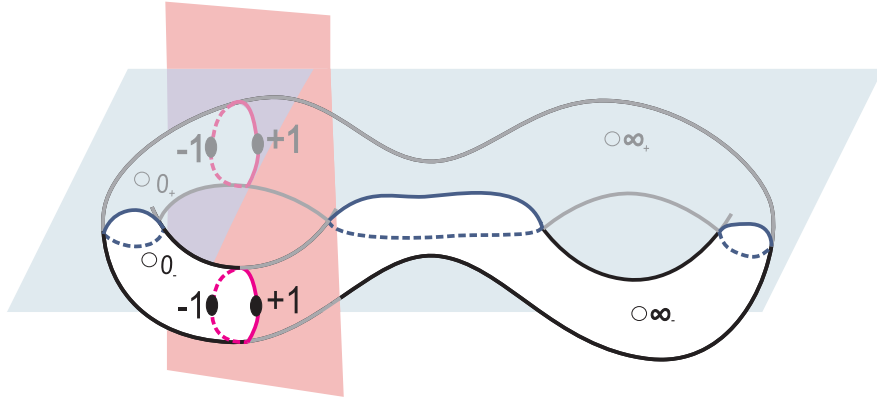


Figure 5: The curves appearing from the finite gap method and the Bethe ansatz equations turn out to be the different projection of the same curve.

Since, by definition,  $p_2 = -p_1$  and  $p_4 = -p_3$  we see that  $p_{3,4}$  describe the exterior of the unit circle in the upper (lower) sheet while  $p_{2,1}$  describe the interior of the unit circle in the upper (lower) sheet.

Comparing the singularities at  $x = \pm 1$  after the map we see that they are again given, due to eq.(3.34), by the energy and momentum in terms of  $\kappa_{\pm}$  in full correspondence with the finite gap result eq.(2.28).

Under this map the 4 infinities of the 4 sheets of quasi-momenta  $p_1, p_2, p_3, p_4$ , fig.3, are mapped according to (see (4.2,4.3))

$$(\infty_{2,1}, \infty_{3,4}) \longleftrightarrow (0_{\pm}, \infty_{\pm}) .$$

Then, from the first line of (3.32), we read off the behavior of the quasi-momenta near  $x = 0_{\pm}$  while from the second line of (3.32) we infer the behavior of the quasi-momenta at  $x = \infty_{\pm}$ . They match the asymptotics (2.27) and (2.26) respectively after imposing  $M = \frac{\sqrt{\lambda}}{4\pi}$  or

$$-\log \mu = \frac{\sqrt{\lambda}}{2}, \quad (4.4)$$

a simple and nice relation exhibiting the dimensional transmutation property of the asymptotically free theory with the precise coefficient<sup>10</sup>.

The filling fractions (3.33) coincide with (2.34) of the finite gap solution since they are homomorphic integrals, invariant w.r.t. the change of projection<sup>11</sup>. The same can be said about the Bethe equations eq.(3.31) which we have to compare with the finite gap equations (2.33), with the following definition of the mode numbers

$$n_i^u = 2m - n_i, \quad n_i^v = n_i. \quad (4.5)$$

<sup>10</sup>For the  $O(N)$  sigma model the beta function for the coupling is given by  $\beta \equiv \frac{\partial}{\partial \log \Lambda} \sqrt{\lambda(\Lambda)} = N - 2$  where  $\Lambda$  is the cutoff of the theory. The dynamically generated mass must be of the form  $m = \Lambda f(\sqrt{\lambda})$ . The functional form of  $f$  is fixed by the  $\beta$  function upon imposing independence on the cutoff of this physical quantity. Thus, for general  $N$ ,  $-\log \mu = \frac{\sqrt{\lambda}}{N-2} + \mathcal{O}(1)$ .

<sup>11</sup>The minus sign in (2.34) comes from relation (4.3) between  $p_1(z)$  and  $\tilde{p}(x)$ .

This redefinition is due to the fact that a  $B_u$ -cycles of eq.(3.32) going from  $\infty_1$  on the upper sheet of fig.3 through the  $u$ -cut to  $\infty_2$  on the next sheet, are projected by Zhukovsky map into the interior of the unit circle of the  $x$  projection, fig.4, with the  $\infty_{1,2}$  projected to  $0_{\mp}$ . To complete it to the  $B$ -cycles as defined in eq.(2.33) we have to complete them with paths  $(\infty_-, 0_-)$  and  $(0_+, \infty_+)$ , each of them is equal to quasi-momentum  $-\tilde{p}(0) = -2\pi m$ . This completed cycle will run in the opposite direction of a usual  $B_k$  cycle, hence the minus sign in eq.(4.5).

The third equation eq.(3.31) follows immediately since integral over the  $B_\theta$ -cycle is mapped into the integral from  $\infty_+$  to  $0_+$  yielding  $\tilde{p}(0)$  as result.

We conclude that the two projections, one obtained from the quantum Bethe ansatz, the other from the classical finite gap solution, represent the same algebraic curve with the same moduli and thus the underlying solutions (states) completely coincide.

As a result we can express densities of the Bethe roots through classical quasi-momentum  $\tilde{p}(x)$  as<sup>12</sup>

$$\begin{aligned}\rho_v(z(x)) &= \rho(x), & x \in C^v \\ \rho_u(z(x)) &= \rho(x), & x \in C^u \\ \rho_\theta(2 \cos \phi) &= -\frac{1}{\pi} \text{Im} \left[ \tilde{p} \left( e^{i\phi} \right) \right], & \phi \in [0, \pi]\end{aligned}$$

where  $2\pi i \rho(x) = \tilde{p}(x - i0) - \tilde{p}(x + i0)$ . These densities automatically satisfy Bethe ansatz equations eq.(3.16).

In Appendix B we provide an alternative, completely algebraic, derivation of the equivalence between the curves.

## 5 Some Limiting Solutions of the Quantum $O(n)$ Sigma-Model

Here we will consider three limiting cases: the BMN solutions from the quantum Bethe equations, the semi-classical solutions with small longitudinal amplitudes and the discrete spin chain limit.

### 5.1 BMN Limit

In this section we will consider the BMN limit [72] which, in our notations, reads  $M \sim L \gg 1$ ,  $J_v, J_u \sim 1$ . We are therefore considering a big  $\theta$  cut which will be slightly perturbed by some point like microscopic  $u$  and  $v$  cuts, treated as corrections. The position of these microscopic cuts in the presence of the  $\theta$  cut are found from the first and third equations in (3.15) with  $G_\theta$  given by (3.19) with  $m = 0$  (the only choice compatible with the stringy condition  $P = 0$  for

---

<sup>12</sup>Last expression deserves some words. Points  $z \pm i0$  below and above the  $\theta$  cut are mapped to  $x = x_+(z)$  and  $x = x_-(z) = 1/x_+(z)$  Since  $z \in [-2, 2]$  these are conjugate points in the unit circle. Then the discontinuity of  $p(z)$  in the  $\theta$  cut is given by the imaginary part of  $\tilde{p}(x)$ .

very small filling fractions for  $u$ 's and  $v$ 's.). We find

$$\frac{L}{M} \frac{1}{\sqrt{x_n^2 - 4}} = 2\pi n, \quad x_n = \text{sign } n \sqrt{4 + \frac{L^2}{4\pi^2 M^2 n^2}}.$$

Then, from the second equation in (3.15), we can compute the correction  $\delta G_\theta$  to the resolvent of the main cut,

$$\delta \mathcal{G}'_\theta(x) = \sum_n \frac{N_n}{x - x_n}$$

where  $N_n = J_n/M$ . Since

$$\delta G_\theta(x) = \delta \mathcal{G}'_\theta(x) + i\pi \delta \rho_\theta(x)$$

we have

$$\delta \rho_\theta(x) = \sum_n N_n \left( \frac{\sqrt{x_n^2 - 4} \text{sign } x_n}{\pi \sqrt{4 - x^2} (x - x_n)} + \frac{1}{\pi \sqrt{4 - x^2}} \right). \quad (5.6)$$

Let us explain why. The inverse square roots follows from the known support and behavior of  $\rho$  near the walls. Then the first term inside the brackets follows from cancellation of the poles at  $x_n$  in  $\delta G_\theta$ . Finally the second term is fixed by requiring  $\mathcal{O}(1/x^2)$  decay of  $\delta G_\theta$  at infinity, or, equivalently, from requiring that the perturbation of the density does not change number of particles in the cut,  $\int \delta \rho_\theta = 0$ .

From (5.6) we can read the change in the behavior near  $\pm 2$  of the density of rapidities, i.e. compute  $\delta \kappa_\pm$  and, therefore,

$$\delta P = 2\pi M \kappa (\delta \kappa_+ - \delta \kappa_-) = - \sum_n n J_n \quad (5.7)$$

$$\delta E = 2\pi M \kappa (\delta \kappa_+ + \delta \kappa_-) = \frac{L}{\sqrt{\lambda}} \sum_n J_n \left( 1 - \sqrt{1 + \frac{\lambda n^2}{L^2}} \right). \quad (5.8)$$

The same result was obtained in [19], but in a different regime, the semi-classical one, where  $1 \ll J_v, J_u \ll L \sim M$ . In our case  $J_n$  are small *integers* which reflects the quantum nature of the result, as for the original BMN result [72].

## 5.2 Multi Cut Vacuum States

In this section we will try to understand the meaning of the multi-cut solutions in  $\theta$  and its possible relation with Virasoro constraint.

We will consider here the solutions in the Abelian  $U(1)$  sector described only by  $\theta$ -variables:

$$g = \exp \left[ -i\tau_3 \left( T\tau + S\sigma + \sum_{\omega > 0} A_\omega \cos(\omega(\tau + \sigma)) + \sum_{\omega < 0} A_\omega \cos(\omega(\tau - \sigma)) \right) \right] \quad (5.9)$$

where  $S$  is the winding number, integer to ensure the periodicity in  $\sigma$ , and  $T = Q_R/\sqrt{\lambda}$  is the angular momentum. For small amplitudes  $A_m$  we can quantize this solution as a set of oscillators. The energy in this approximation reads

$$E = \frac{S^2 \sqrt{\lambda}}{2} + \frac{Q_R^2}{2\sqrt{\lambda}} + \sum_{\omega \neq 0} |\omega| N_\omega \quad (5.10)$$

where  $N_\omega$  is the mode number of the oscillator with the frequency  $\omega$ . This formula is a well known expression for the spectrum of  $U(1)$  model. It is very natural since we can use arguments of BMN to see that in the limit of large angular momentum the system feels only a small neighborhood of the main circle on  $S^3$  and the longitudinal oscillations are described by a massless scalar field. This is why our analysis is only valid for small amplitudes  $A_m$ .

The worldsheet momentum is

$$P = \sqrt{\lambda} ST + \mathcal{O}(1). \quad (5.11)$$

The terms  $\mathcal{O}(1)$  represent quantum corrections which are not captured by the leading semi-classical approximation.

We will show that the solution eq.(5.9) with small amplitudes corresponds to a multi-cut configuration of  $\theta$ 's when all cuts except one are small (with filling fractions of the order 1). We will denote by  $m_0$  the mode number of the large cut and by  $L_{m_0}$  the number of  $\theta$ 's in this cut. We assume  $L_0 \sim \sqrt{\lambda}$ .

We can compute the momentum and the charge in terms of the Bethe ansatz quantities

$$P = m_0 L_{m_0} + \sum_{m \neq m_0} m L_m, \quad Q_R = L_{m_0} + \sum_{m \neq m_0} L_m \equiv L \quad (5.12)$$

and thus

$$T = \frac{L}{\sqrt{\lambda}}, \quad S = m_0 \quad (5.13)$$

where we are allowed to drop  $1/L_0 \sim 1/\sqrt{\lambda}$  terms due to the winding number quantization,  $S \in \mathbb{Z}$ . Having identified  $S$  and  $T$  in the language of Bethe ansatz we can write

$$E = \frac{m_0^2 \sqrt{\lambda}}{2} + \frac{L^2}{2\sqrt{\lambda}} + \sum_{\omega \neq 0} |\omega| N_\omega \quad (5.14)$$

where  $m_0$  and  $L$  are integers. It is left to identify the amplitudes with the remaining filling fraction. Let us denote  $N_\omega = L_{\omega+m_0}$ , then we have

$$E = E_0 + \sum_{m \neq m_0} |m - m_0| L_m. \quad (5.15)$$

Expression (5.14) can also be established from the Bethe ansatz side. One has, see section (3.3), equation (3.24)

$$E = \frac{i}{\pi} \sum_{\zeta_\beta < 0 < \zeta_\alpha} \log S_0^2(M[\xi_\alpha - \xi_\beta]) + \sum_{\alpha} m_\alpha \text{sign}(\xi_\alpha). \quad (5.16)$$

The main cut with the mode number  $m_0$  occupies most of the box. Other cuts are squeezed close to the right (left) wall for  $m_i$  greater (smaller) than  $m_0$ . Then the second term in (5.16) reads

$$\sum_{\alpha} m_\alpha \text{sign}(\xi_\alpha) = \sum_{\alpha} m_0 \text{sign}(\xi_\alpha) + \sum_m |m - m_0| L_m \quad (5.17)$$

We only have to show that the change in the first term in (5.16) and in the first term in (5.17) is small compared to the last term of (5.17). We will demonstrate that the change in one of the mode numbers leads to  $1/L$  displacements of  $\theta$ 's. Consider for example the situation when we decrease the mode number of the first  $\theta$  by  $\delta n \sim 1$ . This  $\theta$  has the biggest displacement since the force acting on it increases by  $2\pi\delta n$ . All other  $\theta$ 's are affected only due to the displacement of the first one. Let us estimate this displacement assuming it to be small. Then one has the following equilibrium condition

$$\pi\mu \cosh(\pi\theta_1)\delta\theta_1 \sim 1. \quad (5.18)$$

Since  $\pi\mu \cosh(\pi\theta_1) \gg 1$ <sup>13</sup> the displacement is small  $\delta\theta \ll 1$ , then  $\delta\xi \ll 1/L$ . This means that the change of the density is negligible  $\delta\rho(\zeta) \ll 1/L$  and we can say that the first term in (5.16) remains intact.

We obtain the precise agreement between semi-classics and Bethe ansatz calculations for several  $\theta$  cuts. We can conclude that the longitudinal oscillations, which break the Virasoro conditions and thus being inadmissible in the string context, manifest themselves as extra cuts in  $\theta$ . We observe indeed this phenomenon, at least when these oscillations are small. As it was said already in the introduction, we conjecture on the base of these arguments and of the comparison of our classical limit with the direct finite gap approach that the Virasoro conditions impose the selection rule on the states described by (3.4,3.5) under which only the solutions having  $\theta_k$ 's with the same mode numbers  $m_1 = \dots = m_L$  are retained.

### 5.3 XXX Spin Chain Limit

In this section we will consider the XXX spin chain limit of the Bethe equations for the principal chiral field. Contrary to the classical limit considered above it is rather a strong coupling limit. Namely, we take  $\mu \rightarrow \infty$  and arbitrary  $L, J_v, J_u$ . In this limit  $\theta$ 's are squeezed near zero. In the leading order we can just take them equal to zero so that (3.5,3.6) become non-interacting two  $SU(2)$  XXX chains

$$\left(\frac{u_j + i/2}{u_j - i/2}\right)^L = \prod_{i \neq j} \frac{u_j - u_i + i}{u_j - u_i - i}, \quad (5.19)$$

$$\left(\frac{v_k + i/2}{v_k - i/2}\right)^L = \prod_{l \neq k} \frac{v_k - v_l + i}{v_k - v_l - i}. \quad (5.20)$$

These equations look similar to the  $\mathcal{N} = 4$  SYM XXX spin chain Bethe equations, the first one for the sector of  $X, Y$  scalars and the second for  $\bar{X}, \bar{Y}$  scalars. To make a more precise comparison we have to fix the conserved quantities. Let us first introduce the notations

$$e_s(u) \equiv i \log \frac{u + is/2}{u - is/2},$$

---

<sup>13</sup>We know that  $E = \frac{1}{2\pi}\mu \sum_{\alpha} \cosh \pi\theta_{\alpha} \sim L$ . With exponential precision we can sum only up  $\theta_{\alpha} < -2M + L^{1/2}$  so that number of terms is of order  $L^{1/4}$  as one easily sees from the density computed in 3.20. Then we have  $E < \mu \cosh(\pi\theta_1)L^{1/4}$  which means  $\mu \cosh(\pi\theta_1) \gg 1$

and

$$\theta_\alpha = \frac{1}{\mu} \theta_\alpha^0 + \frac{1}{\mu^2} \theta_\alpha^1 + \dots$$

Below we will show that energy of the system given by eq.(3.9) is proportional to that of the XXX spin chain

$$E_{\text{xxx}} = \sum_j \frac{1}{u_j^2 + 1/4} + \sum_k \frac{1}{v_k^2 + 1/4}. \quad (5.21)$$

To see this we expand further in powers of  $\mu$ . The formula for energy with  $\mathcal{O}(\theta^3)$  precision becomes

$$E \simeq \frac{\mu}{2\pi} \sum_{\alpha=1}^L \left( 1 + \frac{\pi^2 \theta_\alpha^2}{2} \right). \quad (5.22)$$

Let us evaluate  $\theta^0$  and  $\theta^1$ . We expand BAE (3.4) in powers of  $\theta$  up to  $\mathcal{O}(\theta^3)$

$$\begin{aligned} \mu \sinh \pi \theta_\alpha &\simeq 2\pi m + \sum_{\beta \neq \alpha}^L (\pi \operatorname{sign}(\theta_\alpha - \theta_\beta) - 4(\theta_\alpha - \theta_\beta) \log 2) \\ &- \sum_k e_1(v_k) - \sum_j e_1(u_j) + \theta_\alpha E_{\text{xxx}} + \mathcal{O}(\theta^3). \end{aligned} \quad (5.23)$$

The second term in the r.h.s comes from the expansion of  $S_0$ . Expanding eqs.(3.5,3.6) we have

$$2\pi n_j^u = L e_1(u_j) - L \sum_{i \neq j} e_2(u_j - u_i) - e_1'(u_j) \sum_\alpha \theta_\alpha + \mathcal{O}(\theta^3), \quad (5.24)$$

$$2\pi n_k^v = L e_1(v_k) - L \sum_{l \neq k} e_2(v_k - v_l) - e_1'(v_k) \sum_\alpha \theta_\alpha + \mathcal{O}(\theta^3). \quad (5.25)$$

Summing all eqs.(5.24,5.25), using the level matching condition  $P = 0$  and eq.(5.23) one obtains

$$\mu \pi \theta_\alpha \simeq \pi(2\alpha - L - 1) + \left( \theta_\alpha - \frac{1}{L} \sum_\beta \theta_\beta \right) (E_{\text{xxx}} - 4L \log 2) + \mathcal{O}(\theta^3), \quad (5.26)$$

so that

$$\theta_\alpha^0 = 2\alpha - L - 1, \quad \theta_\alpha^1 = \theta_\alpha^0 (E_{\text{xxx}} - 4L \log 2)$$

and thus, from eq.(5.22),

$$E = \left[ \frac{L\mu}{2\pi} + \frac{\pi L(L^2 - 1)}{12\mu} - \frac{2\pi L^2(L^2 - 1)}{3\mu^2} \log 2 \right] + \left[ \frac{\pi L(L^2 - 1)}{6\mu^2} \right] E_{\text{xxx}}. \quad (5.27)$$

This formula, together with eq.(5.19), reproduces the energy and the Bethe equations for the XXX spin chain up to the constant terms inside the square brackets. Although it is known that the perturbative expansion of the energy  $E$  in general does not coincide with that of the eigenvalue of the dilatation operator in SYM [28], it has been confirmed that they coincide up to two-loop approximation in the continuous limit [19]. The above result may serve as a starting point to elucidate the matching at the discrete level.

## 6 $O(6)$ Sigma-Model

Let us now move on to a larger subsector of the superstring theory, namely let us consider the  $O(6)$  non-linear sigma model. As before we describe a general quantum state by the system of vector particles which live on a circle of length  $\mathcal{L} = 2\pi$ . The wave function is then specified by a set of rapidities  $\{\theta_\alpha\}$  which determine the coordinate part of the wave function, plus a set of Bethe roots  $\{u_j^{(1)}, u_j^{(2)}, u_j^{(3)}\}$  encoding its color structure<sup>14</sup>. When imposing periodicity of the wave function one obtains the quantization of these parameters. They are constrained by Bethe ansatz equations (see Appendix D for the derivation and for the generalization to  $O(2n)$ )

$$\begin{aligned}
e^{-i\mu \sinh \frac{\pi\theta_\alpha}{2}} &= \prod_{\beta \neq \alpha}^L S_0(\theta_\alpha - \theta_\beta) \prod_{j=1}^{K_2} \frac{\theta_\alpha - u_j^{(2)} + i/2}{\theta_\alpha - u_j^{(2)} - i/2} \\
1 &= \prod_{j \neq i}^{K_1} \frac{u_i^{(1)} - u_j^{(1)} + i}{u_i^{(1)} - u_j^{(1)} - i} \prod_{j=1}^{K_2} \frac{u_i^{(1)} - u_j^{(2)} - i/2}{u_i^{(1)} - u_j^{(2)} + i/2} \\
\prod_{\alpha=1}^L \frac{u_i^{(2)} - \theta_\alpha + i/2}{u_i^{(2)} - \theta_\alpha - i/2} &= \prod_{j \neq i}^{K_2} \frac{u_i^{(2)} - u_j^{(2)} + i}{u_i^{(2)} - u_j^{(2)} - i} \prod_{j=1}^{K_3} \frac{u_i^{(2)} - u_j^{(3)} - i/2}{u_i^{(2)} - u_j^{(3)} + i/2} \prod_{j=1}^{K_1} \frac{u_i^{(2)} - u_j^{(1)} - i/2}{u_i^{(2)} - u_j^{(1)} + i/2} \\
1 &= \prod_{j \neq i}^{K_3} \frac{u_i^{(3)} - u_j^{(3)} + i}{u_i^{(3)} - u_j^{(3)} - i} \prod_{j=1}^{K_2} \frac{u_i^{(3)} - u_j^{(2)} - i/2}{u_i^{(3)} - u_j^{(2)} + i/2}
\end{aligned} \tag{6.1}$$

where

$$S_0(\theta) = -\frac{\Gamma\left(\frac{1}{4} - i\frac{\theta}{4}\right) \Gamma\left(\frac{1}{2} - i\frac{\theta}{4}\right) \Gamma\left(\frac{3}{4} + i\frac{\theta}{4}\right) \Gamma\left(1 + i\frac{\theta}{4}\right)}{\Gamma\left(\frac{1}{4} + i\frac{\theta}{4}\right) \Gamma\left(\frac{1}{2} + i\frac{\theta}{4}\right) \Gamma\left(\frac{3}{4} - i\frac{\theta}{4}\right) \Gamma\left(1 - i\frac{\theta}{4}\right)}. \tag{6.2}$$

In the next subsection we will show that, in the classical scaling limit  $L \sim \log \frac{1}{\mu} \rightarrow \infty$ , the solutions of this system of Bethe ansatz equations are in one to one correspondence with classical solutions of  $O(6)$  sigma model, classified by means of an algebraic curve [21]. The derivation here will be similar to the  $SU(2)$  principal chiral field considered in previous section. In the classical limit when  $\theta$ 's will be large we can use Coulomb approximation and substitute  $S_0(\theta)$  by its large  $\theta$  asymptotics

$$i \log S_0(\theta) = \frac{1}{\theta} + \mathcal{O}(1/\theta^3).$$

Furthermore, the potential becomes a square box and  $\theta_\alpha/M$  will therefore be distributed, at leading order, between  $-2$  and  $2$  provided we define the variable  $z = \theta/M$  with  $M = -\frac{\log \mu}{\pi}$ . Thus, in this limit, we can recast (6.1) as

$$\begin{aligned}
2\mathcal{G}'_1 - G_2 &= 2\pi n^{(1)} \\
2\mathcal{G}'_2 - G_1 - G_3 - G_\theta &= 2\pi n^{(2)}, & \mathcal{G}'_\theta - G_2 &= 2\pi m \\
2\mathcal{G}'_3 - G_2 &= 2\pi n^{(3)}
\end{aligned} \tag{6.3}$$

---

<sup>14</sup>For a general simple group one would have  $r$  different kinds of roots where  $r$  is the rank of the group, i.e. the number of simple roots.

where the resolvents are given by

$$G_\theta(z) = \frac{1}{M} \sum_\alpha \frac{1}{z - \theta_\alpha/M}, \quad G_l(z) = \frac{1}{M} \sum_i^{K_l} \frac{1}{z - u^{(i)}/M}, \quad l = 1, \dots, 3, \quad (6.4)$$

and each equation holds for  $z$  belonging to a  $\theta$  or  $u^{(i)}$  cut if  $G_\theta$  or  $G_i$  is slashed, respectively. These equations, as we will show in the next subsection, can be used to define some algebraic curve which maps onto the classical curve of [21] after Z-transformation  $z = x + 1/x$ .

The quantum state (Bethe vector) corresponding to the solutions of (6.1) carries the following  $\mathfrak{so}(6)$  spins

$$\begin{aligned} J_1 &= L - K_2, \\ J_2 &= K_2 - K_1 - K_3, \\ J_3 &= K_1 - K_3, \end{aligned} \quad (6.5)$$

where  $(J_1, J_2, J_3)$  are measured by the orthonormal basis of the Cartan subalgebra.

## 6.1 Algebraic Curve

To relate solutions of BAE (6.1) with classical solutions classified by algebraic curves [21] we will construct possible curves corresponding to (6.3). This means that the resolvents  $G_{1,2,3}(z)$  and  $G_\theta(z)$ , when taken in appropriate linear combinations, are in fact different branches of some unique analytical function. In fact there are several possible combinations, each of them corresponding to different representation of  $SO(6)$ .

### 6.1.1 Curve for the Vector Representation

The curve in vector representation is the most simple one. Introducing quasi-momenta

$$\begin{aligned} q_1 &= G_\theta - G_2 \\ q_2 &= G_2 - G_3 - G_1 \\ q_3 &= G_1 - G_3 \end{aligned} \quad (6.6)$$

one can easily see from eq.(6.3) that  $(q'_{1,2,3}, -q'_{1,2,3})$  are branches of the same function. Riemann surface corresponding to this function is depicted in fig.6, to the right. In terms of these quasi-momenta eq.(6.3) takes the form

$$\begin{aligned} \not{q}_1 - \not{q}_2 &= 2\pi n^{(2)} \\ \not{q}_3 - \not{q}_2 &= 2\pi n^{(1)}, \quad \not{q}_1 = 2\pi m \\ \not{q}_2 + \not{q}_3 &= -2\pi n^{(3)} \end{aligned} \quad (6.7)$$



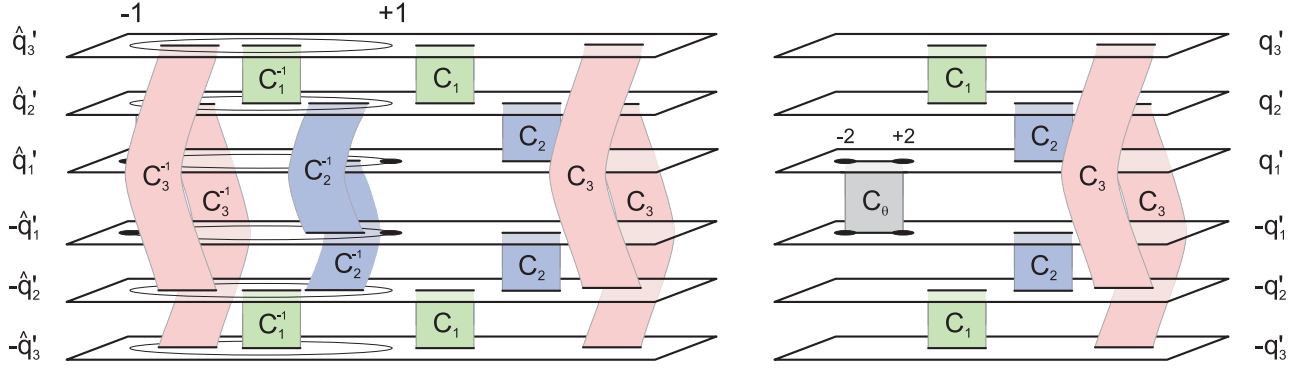


Figure 6: Riemann surfaces resulting from classics and from the Bethe ansatz match after Zhukovsky map. On the left picture we plot some possible cuts coming from the classical curves analysis, (2.17). For each cut outside the unit circle there is a mirror cut inside the unit circle, (6.10). In this picture we did not plot some possible cuts, for sake of simplicity. There is no cut, for instance connecting  $q_1$  and  $q_3$ . On the right picture we present the curve obtained from the Bethe ansatz point of view, (6.7). Here it might seem that we have plotted every possible type of cuts. It is not the case – due to the existence of stacks [24] roots of different kinds can attract each other forming some extra cuts. This extra cuts would be the image, under Zhukovsky map, of the cuts which we did not plot on the left figure.

Let us see how this curve appears from the results of [21], reviewed in Section 2.2. There one has the curve  $(\hat{q}'_1, \hat{q}'_2, \hat{q}'_3, -\hat{q}'_1, -\hat{q}'_2, -\hat{q}'_3)$  with the properties (2.14,2.15,2.16),

$$\hat{q}_k(x) = \delta_{k=1} \frac{2\pi \kappa_{\pm}}{x \mp 1} + \mathcal{O}(1), \quad (6.8)$$

$$\hat{q}_k(x) = \frac{4\pi J_k}{\sqrt{\lambda}} \frac{1}{x} + \mathcal{O}(1/x^2), \quad (6.9)$$

$$\hat{q}_k(1/x) = \delta_{k,1} (4\pi m - \hat{q}_1(x)) + (1 - \delta_{k,1}) \hat{q}_k(x). \quad (6.10)$$

Charges  $J_i$  are properly normalized to be integers.

Let us check that Z-transformation maps this classical curve to the curve (6.6) corresponding to a solution of BAE (6.1). Namely<sup>15</sup>

$$q_k(z) = \hat{q}_k(x_+) \quad x_+ = \frac{1}{2} \left( z + \sqrt{z^2 - 4} \right). \quad (6.11)$$

Where the square root is defined in such a way that  $|x_+| > 1$  for  $z \in \mathbb{C}$ . Since the values of  $\hat{q}_i$  inside the unit circle are related with the values of  $\hat{q}_i$  outside unit circle by eq.(6.10) we can always reconstruct  $\hat{q}(x)$  in the whole  $x$  plane from  $q(z)$ . From (6.8,6.10), one has, for small  $\epsilon$ ,

$$\hat{q}_1(1 + \epsilon) = 2\pi m + \frac{2\pi \kappa_+}{\epsilon} + \sum_{k=1}^{\infty} C_k^{(1)} \epsilon^{2k-1} \quad (6.12)$$

$$\hat{q}_{2,3}(1 + \epsilon) = \sum_{k=0}^{\infty} C_k^{(2,3)} \epsilon^{2k} \quad (6.13)$$

<sup>15</sup>We notice that this is the only possible normalization – (6.7) and (2.17) forbid us to multiply  $q_k$  by any constant coefficient.

Since, after Zhukovsky map,  $q_k(2 + \epsilon) = \hat{q}_k(1 + \sqrt{\epsilon})$ , one sees that a new cut appears connecting  $\pm q'_1$  while no singularity appears for  $q'_{2,3}$  (see fig.6). This is consistent with eq.(6.6) where only  $q_1$  has  $\theta$  cut.

Let us now understand this Z-map in greater detail. We start with six sheets  $(\pm \hat{q}'_{1,2,3})$ . Then we apply Zhukovsky map by means of which each of these sheets is mapped to a new pair of sheets, one coming from points located originally inside the unit circle while the other is the map of the points in the exterior. We designate this set of sheets by  $(\pm q'^{in}_{1,2,3}, \pm q'^{out}_{1,2,3})$ . Now, from (6.10), we know that,

$$(\mp q'^{out}_1, \mp q'^{out}_{2,3}) = (\pm q'^{in}_1, \mp q'^{in}_{2,3}).$$

Thus we can keep only the sheets in the left hand side. Their cut structure, figure 6, is inherited from the original ones with an additional cut between  $\pm q'_1$  as explained above. It is exactly the structure we find from the BAE point of view (6.6).

A small remark is in order here. From (2.17) we see that classical curve can have more cuts than are listed in eq.(6.7) and depicted in fig. 6. For example  $\hat{q}'_1$  and  $\hat{q}'_3$  can be connected by a cut. This apparent discrepancy is solved by the introduction of stacks [24]. In the thermodynamical limit Bethe roots of different types can group near the same extremum and form cuts. To describe them one can also define resolvents. As a result, quasi-momenta eq.(6.6) can have cuts connecting for example  $q_1$  and  $q_3$ . For more details see [24], Section 4.

It is now clear, that the equations in the first row in (6.7) follow from (2.17) using the map (6.11). It is also the case for the equation to the right row. Indeed, from eq.(6.10), one has

$$2\hat{q}_1(z) = q_1(z + i0) + q_1(z - i0) = \hat{q}_1(x_+[z + i0]) + \hat{q}_1(x_+[z - i0]) = 4\pi m \quad (6.14)$$

where for the last equality we use  $x_+(z + i0) = 1/x_+(z - i0)$ . Other equalities are just restatements of our definitions.

From (6.12,6.13) and (6.6) we see that

$$\rho_\theta \equiv -\frac{1}{2\pi i} (G_\theta(z + i0) - G_\theta(z - i0)) \simeq \frac{2\kappa_\pm}{\sqrt{2 \mp z}}, \quad z \rightarrow \pm 2 \quad (6.15)$$

Now, having related  $q_{1,2,3}(z)$  and  $\hat{q}_{1,2,3}(x)$  we can relate  $\sqrt{\lambda}$  and  $M$ . Namely from the definitions (6.6,6.4) we immediately see that, for large  $z$ ,

$$\begin{aligned} q_1(z) &\simeq \frac{1}{z} \frac{L - K_2}{M}, \\ q_2(z) &\simeq \frac{1}{z} \frac{K_2 - K_3 - K_1}{M}, \\ q_3(z) &\simeq \frac{1}{z} \frac{K_1 - K_3}{M}. \end{aligned} \quad (6.16)$$

Comparing with (6.9,6.5) we obtain  $M = \frac{\sqrt{\lambda}}{4\pi}$  or, since  $M = -\frac{\log \mu}{\pi}$ ,

$$-\log \mu = \frac{\sqrt{\lambda}}{4}. \quad (6.17)$$

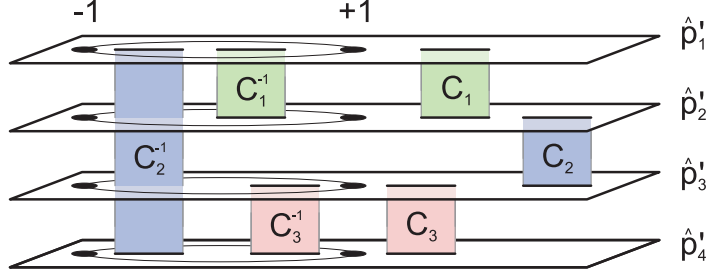


Figure 7: Classical curve from [21]. For each cut outside the unit circle there is a mirror cut inside the unit circle – eq.(6.22). In each sheet there are poles at  $\pm 1$  which will lead to  $\theta$  cuts after  $Z$ -transformation – see fig.8.

This result matches perfectly the 1-loop  $\beta$ -function of  $O(6)$  sigma model (see footnote in Section 4). It is a strong confirmation of our correspondence between the quantum Bethe ansatz eq.(6.1) in the scaling limit and the classical sigma model.

### 6.1.2 Curve for the Spinor Representation

In this subsection we will construct the curve associated with the spinor representation. Having already seen the mechanism at work in the previous section we will now proceed rather briefly. An 8-sheet surface can be build by introducing quasi-momenta

$$\begin{aligned}
p_1 &= \frac{1}{2} G_\theta - G_1 \\
p_2 &= \frac{1}{2} G_\theta + G_1 - G_2 \\
p_3 &= -\frac{1}{2} G_\theta - G_3 + G_2 \\
p_4 &= -\frac{1}{2} G_\theta + G_3.
\end{aligned} \tag{6.18}$$

It is then easy to see that  $(p'_{1,2,3,4}, -p'_{1,2,3,4})$  are branches of the same analytical function (see fig.8). Indeed

$$\begin{aligned}
p'_1 - p'_2|_{C_1} &= -2\mathcal{G}'_1 + G'_2 = 0 \\
p'_1 + p'_2|_{C_\theta} &= \mathcal{G}'_\theta - G'_1 = 0 \\
p'_2 - p'_3|_{C_2} &= -2\mathcal{G}'_2 + G'_\theta + G'_1 + G'_3 = 0 \\
p'_3 + p'_4|_{C_\theta} &= -\mathcal{G}'_\theta + G'_3 = 0 \\
p'_3 - p'_4|_{C_3} &= -2\mathcal{G}'_3 + G'_2 = 0
\end{aligned} \tag{6.19}$$

This curve corresponds to the classical curve in spinor representation [21]. As in the previous subsection they are related by  $Z$ -transformation (see fig.7). After Zhukovsky transformation 4 sheets split into 8. Since there are poles at  $\pm 1$  in each of the original 4 sheets the resulting 8 sheets will be pairwise connected by 4  $\theta$  cuts as shown in fig.8.

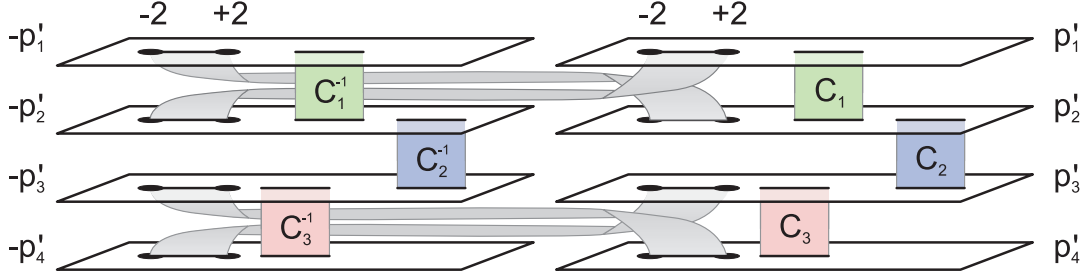


Figure 8: Curve corresponding to the classical limit of the quantum Bethe ansatz. It is related by Z-transformation with the curve on fig.7.

Let us use the spinor curves to relate  $M$  and  $\sqrt{\lambda}$  as in previous subsection. The vector representation (of the previous subsection) and the spinor representation are related by [21]

$$\begin{aligned} p_1 &= \frac{q_1 + q_2 - q_3}{2}, & p_2 &= \frac{q_1 - q_2 + q_3}{2} \\ p_3 &= \frac{-q_1 + q_2 + q_3}{2}, & p_4 &= \frac{-q_1 - q_2 - q_3}{2}, \end{aligned}$$

with the same expression for hatted quantities. Then the properties for the  $\hat{q}$ 's lead to

$$\begin{aligned} \hat{p}_1(1/\epsilon) &\simeq \frac{2\pi\epsilon}{\sqrt{\lambda}}(J_1 + J_2 - J_3), & \hat{p}_2(1/\epsilon) &\simeq \frac{2\pi\epsilon}{\sqrt{\lambda}}(J_1 + J_3 - J_2) \\ \hat{p}_3(1/\epsilon) &\simeq \frac{2\pi\epsilon}{\sqrt{\lambda}}(J_2 + J_3 - J_1), & \hat{p}_4(1/\epsilon) &\simeq -\frac{2\pi\epsilon}{\sqrt{\lambda}}(J_1 + J_2 + J_3) \end{aligned} \quad (6.20)$$

and

$$\not{p}_k \mp \not{p}_l = 2\pi n_a, \quad x \in C_a. \quad (6.21)$$

Furthermore  $x \leftrightarrow 1/x$  relates different sheets of the surface

$$\hat{p}_{1,2}(1/x) = 2\pi m - \hat{p}_{2,1}(x), \quad \hat{p}_{3,4}(1/x) = -2\pi m - \hat{p}_{4,3}(x) \quad (6.22)$$

Again we state the following relation

$$p_{1,2,3,4}(z) = \hat{p}_{1,2,3,4} \left( \frac{1}{2} \left[ z + \sqrt{z^2 - 4} \right] \right)$$

Now we compute  $p_i$  on  $C_\theta$ . From eq.(6.22) we have equations for  $\theta$ -cut

$$\not{p}_1 + \not{p}_2 = 2\pi m, \quad \not{p}_3 + \not{p}_4 = -2\pi m. \quad (6.23)$$

Among the equations (6.21) one has

$$\begin{aligned} \not{p}_2 - \not{p}_1 &= 2\pi n^{(1)}, & x &\in C_1 \\ \not{p}_3 - \not{p}_2 &= 2\pi n^{(2)}, & x &\in C_2 \\ \not{p}_4 - \not{p}_3 &= 2\pi n^{(3)}, & x &\in C_3 \end{aligned}$$

which give us eq.(6.3). Remaining equations are seen in the Bethe ansatz side through the introduction of stacks (see discussion in previous subsection.). Finally from (6.18) and (6.20) we again obtain (6.17).

## 6.2 Energy and Momentum

In this subsection let us observe the perfect matching of both energy and momentum from classical and Bethe ansatz calculations. Energy is again defined by

$$E = \frac{\mu}{2\pi} \sum_{\alpha} \cosh\left(\frac{\pi\theta_{\alpha}}{2}\right). \quad (6.24)$$

Repeating the same calculations as for  $SO(4)$  case we see that once again the result depends on the behaviour of  $\rho_{\theta}(z)$  near points  $z = \pm 2$ , eq.(6.15). In fact everything goes exactly as before so that we will arrive at the equivalent of (3.38), namely

$$E = 2\pi M \kappa_{-}^2 + \left( - \sum_{a=1,2,3} \sum_p n_p^{(a)} S_p^{(a)} - mL \right).$$

Let us recall that this was obtained by calculating the  $a$  independent integral for  $a = -2 + \epsilon$ . Had we calculated it for  $a = 2 - \epsilon$  and we would have obtained

$$E = 2\pi M \kappa_{+}^2 - \left( - \sum_{a=1,2,3} \sum_p n_p^{(a)} S_p^{(a)} - mL \right).$$

Both results should be equal. This gives us not only the value of the energy

$$E = \pi M (\kappa_{-}^2 + \kappa_{+}^2), \quad (6.25)$$

but also the value of the expression in the parentheses which is nothing but the total momentum  $P$  obtained as before by summing Bethe equations

$$P = \frac{\mu}{2\pi} \sum_{\alpha} \sinh(\pi\theta_{\alpha}) = - \sum_{a=1,2,3} \sum_p n_p^{(a)} S_p^{(a)} - mL = \pi M (\kappa_{+}^2 - \kappa_{-}^2). \quad (6.26)$$

Since we have already identified  $M = \frac{\sqrt{\lambda}}{4\pi}$  we observe perfect matching between (6.25,6.26) and the classics (2.8).

## 7 Conclusions and Prospects

The  $O(2n)$   $\sigma$ -models considered in this paper cannot be viewed of course as string sigma models in its full quantum version, although the  $O(6)$   $\sigma$ -model in the classical scaling limit perfectly describes the compact bosonic sector of classical superstring on  $AdS_5 \times S^5$ , when the Virasoro conditions are imposed. We rather consider these quantum theories as toy models bearing many realistic features of a quantum string sigma model and shedding some light on the quantization of the full Green-Schwarz-Metsaev-Tseytlin superstring. These models show some important features of, yet unknown in full detail, string Bethe equations: the nested nature of these equations, following from the symmetry algebra of the target space, the underlying discrete

quantum degrees of freedom whose role is played in our case by physical particles and by the magnon type excitations on a dynamical inhomogeneous lattice created by particles etc.

Let us point out that the starting point of our construction, the physical S-matrix, can be viewed as describing the anti-ferromagnetic states of a specific inhomogeneous lattice spin chain, as pointed out in [42]<sup>16</sup>, what might be related to the proposals of [37]. The resulting inhomogeneous dynamical spin chain of our paper is however treated in the ferromagnetic way in order to restore the classical limit.

This dynamical lattice becomes regular and rigid in the strong coupling limit of  $\sigma$ -model giving the XXX-type spin chain, similar (up to some normalization factors) to the spin chain describing the 1-loop  $\mathcal{N} = 1$  SYM dilatation operator. This observation might lead to the right mechanism reproducing the all-loop SYM Bethe ansatz of the papers [26, 27, 65], including the periodicity with respect to momentum due to the regular lattice. The Hubbard model interpretation of the paper [65] should be somehow incorporated in the full quantum string.

The asymptotic freedom of the quantum  $O(2n)$  models cannot be a part of this full string  $\sigma$ -model on  $AdS_5 \times S^5$ . It should be rather a finite theory, with zero beta function and without any logarithmic divergencies in the world sheet perturbation theory.

What could this string sigma model look like? We find the construction of quantum string states out of the physical particles based on the Yang periodicity equation of eq.(3.1) very promising. Of course there can be no massive particles there, and the  $\theta$ -filling of the vacuum described here and in [64] should be based not on the confining box potential but on a subtle equilibrium between all roots of the Bethe ansatz equations.

It is plausible to think that the system of Bethe equations for the full theory is based on the  $\mathfrak{psu}(2, 2|4)$  algebra and may look like an affine extension of it, as we saw in the bosonic cases. Even though the scattering of particles in the critical string theory could be qualitatively different from that of massive particles, we still expect that such Bethe ansatz equations may serve as a quasi-particle description [73, 74] and provide us with a basis for the Fock-space like construction of the quantum Hilbert space.

Apart from the string theory applications, we think that our method of restoring the classical limit of integrable sigma models is interesting in itself and can be applied to many problems of two-dimensional field theories, especially for the construction of the quasi-classical approximation. It is also useful for proving the validity of more heuristic approaches to such field theories, like of the Zamolodchikovs' bootstrap S-matrices. In particular, we consider the coincidence of our classical limit in the Bethe ansatz with the finite gap solution of the  $O(2n)$  sigma models as a decisive proof of correctness of the bootstrap approach.

Another interesting possibility based on our observations is the construction of quantization schemes of integrable models starting from the algebraic curves of their finite gap solutions (quantization of KdV system in [75] provides an interesting example). To quantize the algebraic curve, we have to choose its particular projection (Riemann surface) and introduce the Bethe

---

<sup>16</sup>We thank D. Serban for the discussion on this issue.

roots which form the cuts of the Riemann surface in the classical limit. The quantization might be possible in different projections, but some of them should be more convenient than the others. We saw for example from our construction that quantization of the finite gap algebraic curve of  $O(2n)$  sigma model looks more natural after a change of projection by Zhukovsky map.

An interesting application of our methods might be the calculation of quantum  $1/L$  corrections in the compact sector of superstring. It was pointed out in [33] that the direct string calculations of [11] of this effects can be reproduced from the compact sector only by the use of a natural  $\zeta$ -functional regularization, without a direct computation of fermionic contributions. Our Bethe ansatz is a good starting point for such calculation.

### Acknowledgements

We would like to thank I. Kostov, J. Penedones, D. Serban, J. Troost, Al. Zamolodchikov and especially F. Smirnov and K. Zarembo for discussions. The work of V.K. was partially supported by European Union under the RTN contracts MRTN-CT-2004-512194 and by INTAS-03-51-5460 grant. The work of N.G. was partially supported by French Government PhD fellowship and by RSGSS-1124.2003.2. P. V. is supported by the Fundação para a Ciência e Tecnologia fellowship SFRH/BD/17959/2004/0WA9.

### Note Added:

We thank T. Klose and K. Zarembo for informing us on their forthcoming work [76] where they also developed an approach to the quantization of stringy sigma models in various subsectors of the superstring theory on  $AdS_5 \times S^5$ . Their approach seems to be very different from ours, although both give the right classical string limit. Hopefully, both quantizations describe the same system and provide an important complementary information on it.

### Appendix A Charged Particles in a Box

Let us analyse Bethe equations eq.(3.18) with no  $u$ 's nor  $v$ 's present. Furthermore we will considering a single mode number for  $\theta$ 's (which in the continuous limit means only one  $\theta$  cut).

Has we explained in section 3, the  $\mu \cosh M\pi x$  potential is essentially a box when  $\mu = e^{-\frac{M}{2\pi}}$  is small, see figure 1. Furthermore, provided we are considering  $\theta$  roots not to close to the edges of the distribution, i.e. the walls of the box, coulomb interaction in the thermodynamical limit, where  $L \sim M \rightarrow \infty$ , becomes exact.

To gain some intuition about this system we will find exact distribution of the system of Coulomb particles inside square box. For the sake of generality we consider a box will charged walls with charge  $qM$ . Then the equilibrium condition is

$$\frac{1}{M} \sum_{j \neq i} \frac{1}{x_i - x_j} = 2q \frac{x_i}{4 - x_i^2}.$$

The solutions of this discrete equation, i.e. the positions of the particles are the zeros of the Jacobi polynomials [17]. Indeed, defining  $Q(x) = \prod_j (x - x_j)$ , one has

$$\frac{Q''(x_i)}{Q'(x_i)} = 2 \sum_{j \neq i} \frac{1}{x_i - x_j} = 4qM \frac{x_i}{4 - x_i^2},$$

which implies that the  $L$  degree polynomial  $R(x) = Q''(x)(4 - x^2) - 4qMxQ'(x)$  has the same zeros as  $Q(x)$  so they must be the same up to a multiplicative constant. Comparing the  $x^L$  coefficient one finds  $R(x) = (-L(L-1) - 4qML)Q(x)$  so that

$$Q''(x)(4 - x^2) - 4qMxQ'(x) + (L(L-1) + 4qML)Q(x) = 0.$$

Thus

$$Q(x) \propto P_L^{2q-1, 2q-1} \left( \frac{x}{2} \right)$$

where  $P_n^{a,b}(z)$  are the Jacobi polynomials. Particles will be located at the zeros of this polynomials.

Let us analyse the large  $M, L$  limit. From the differential equation for  $Q$  one has, for the resolvent  $G = \frac{1}{M} \frac{Q'}{Q}$ ,

$$\frac{1}{M} \frac{dG(x)}{dx} = -G^2(x) + 4q \frac{x}{4 - x^2} G(x) - \left( \frac{L^2}{M^2} + \frac{4qL}{M} - \frac{L}{M^2} \right) \frac{1}{4 - x^2}.$$

Then in the large  $L \sim M$  limit

$$G(x) = \frac{2qx - 2\sqrt{(2q + \frac{L}{M})^2 x^2 - 4 \left( \frac{L^2}{M^2} + \frac{4qL}{M} \right)}}{4 - x^2}. \quad (\text{A.1})$$

Thus, for small  $q$ , the density has 2 peaked maxima near the walls at  $\pm 2$ . It vanishes before reaching the wall as a square root. In the limiting case, when  $q \rightarrow 0$ , the support goes to  $[-2, 2]$  as expected and the density becomes

$$\rho(x) \rightarrow \frac{1}{\pi \sqrt{4 - x^2}}.$$

which reproduces eq.(3.20) for  $m = 0$  in proper normalization.

We considered this exactly solvable example to demonstrate that influence of the walls results in the inverse square root behavior of the density near the walls.

## Appendix B Relating resolvents

Equivalence between (3.15) and (B.5) will be established in this section. We define resolvents in the  $x$  and  $z$  planes as

$$H_{\pm}(x) \equiv \int_{C_{\pm}} \frac{\rho[y]}{x - y} dy, \quad G_{\pm}(z) \equiv \int_{C_{\pm}} \frac{\rho[y_{\pm}(w)]}{z - w} dw, \quad y_{\pm}(w) = \frac{1}{2} \left( w \pm \sqrt{w^2 - 4} \right) \quad (\text{B.1})$$



where  $C_{\pm}$  are cuts outside (inside) the unit circle in the  $x$  plane. Since

$$G_{\pm}(z) = \int_{C_{\pm}} \frac{\rho[y]}{z - w(y)} w'(y) dy = \int_{C_{\pm}} \rho(y) \left( \frac{1}{x(z) - y} + \frac{1}{y} + \frac{1}{\frac{1}{x(z)} - y} \right) dy \quad (\text{B.2})$$

we have

$$G_{\pm}(z) = H_{\pm}[x_{\pm}(z)] + H_{\pm}[x_{\mp}(z)] - H_{\pm}(0). \quad (\text{B.3})$$

### Derivation of BAE from Classical Equations

It is natural, see (B.3), to define

$$\begin{aligned} G_v(z) &\equiv H_+(x_+) + H_+(x_-) - H_+(0), \\ -G_u(z) &\equiv H_-(x_+) + H_-(x_-) - H_-(0), \\ G_{\theta}(z) &\equiv \frac{4\pi\kappa}{\sqrt{z^2 - 4}} + 2H_+(x_-) - 2H_-(x_+) - 2H_+(0). \end{aligned} \quad (\text{B.4})$$

These functions are indeed resolvents, i.e. they have only cuts and behave as  $1/z$  at infinity. Indeed from  $x_+(\infty) = \infty$ ,  $x_-(\infty) = 0$  we see that they vanish for large  $z$ . Now,  $G_v$  ( $G_u$ ) have only  $v$  ( $u$ ) cuts since at the cut  $[-2, 2]$  one has  $x_+ \leftrightarrow x_-$ . On the other hand  $G_{\theta}(z)$  has only got  $\theta$  cut.

Then, it is easy to see that (3.15) is satisfied if

$$\mathbb{H}(x) = \frac{\pi\kappa}{x-1} + \frac{\pi\kappa}{x+1} + \pi n, \quad H(0) = 2\pi m \quad (\text{B.5})$$

### Derivation of Classical Equations from BAE

Now let us assume that eq.(3.15) is satisfied and let us show that  $H(x)$  defined by

$$H(x_+) \equiv G_v(z) - \frac{G_{\theta}(z)}{2} + \frac{2\pi\kappa}{\sqrt{z^2 - 4}} \quad (\text{B.6})$$

$$H(x_-) \equiv -G_u(z) + \frac{G_{\theta}(z)}{2} - \frac{2\pi\kappa}{\sqrt{z^2 - 4}} + 2\pi m \quad (\text{B.7})$$

satisfies eq.(B.5). To see this it suffices to notice that  $\pm \frac{2}{\sqrt{z^2 - 4}} = \frac{1}{x_{\pm} - 1} + \frac{1}{x_{\pm} + 1}$ . Moreover since  $x_- = 0$  means  $z = \infty$  we immediately have  $H(0) = 2\pi m$ . Since  $\mathcal{G}_{\theta} - G_u - G_v = -2\pi m$ ,  $H(x)$  is continuous on the unit circle and is thus a well defined function of  $x$ . Furthermore it is obviously zero at infinity.

## Appendix C Bootstrap and Bethe Ansatz

To make the account of this paper self-contained, we decided to review in this appendix the original bootstrap program of [38] for the  $SO(4) = SU(2) \times SU(2)$  non-linear sigma model. We follow closely, apart from some minor changes, the original notation. Furthermore we will use the obtained  $S$ -matrix to carry the algebraic Bethe ansatz procedure and quantize the sigma model [71].

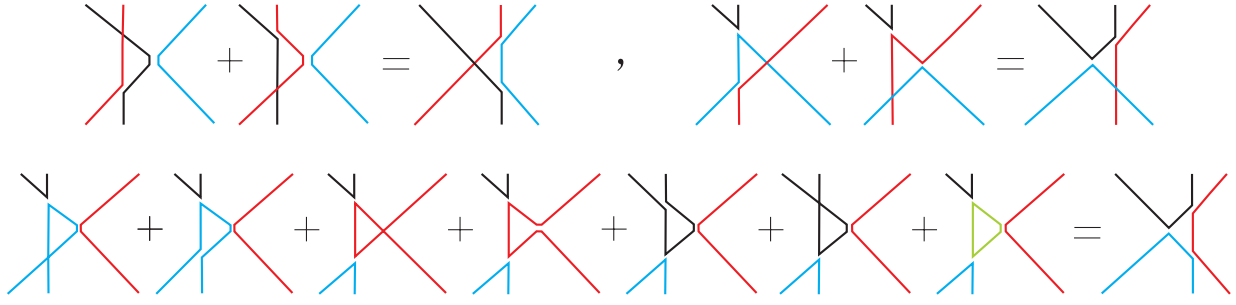


Figure 9: Pictorial representation of Yang Baxter equation. In each diagram time flows in the up direction and initial particles are aligned, from left to right, according to its rapidity (the faster the more to the left). Consider for instance the last diagram in the lhs of the last equation. It represents the annihilation of two blue particles to form any possible pair of green particles. One of the particles of this pair will be reflected back by a red particle to meet again its green twin and annihilate to give rise to a pair of black particles. The fastest “in”-particles are the blue ones while the slowest “out”-particles are the black ones.

Particles are associated to the noncommutative symbols  $A_i(\theta)$  where  $i = 1, \dots, 4$  stands for the isovector index and the rapidity  $\theta$  parametrizes the momentum as  $p = m_0 \cosh(\pi\theta)$ . “In” states are identified with products arranged in the order of decreasing rapidity while “out” states should be arranged in the opposite order. The transition from a 2 particle “in”-state to an “out”-state (assuming no particle creation, which is indeed a condition for integrability) is written as

$$A_i(\theta)A_j(\theta') = S_2(\Delta\theta) \left( g^{-1}(\Delta\theta)\delta_{ij} \sum_{k=1}^4 A_k(\theta')A_k(\theta) + A_j(\theta')A_i(\theta) + h^{-1}(\Delta\theta)A_i(\theta')A_j(\theta) \right) \quad (\text{C.1})$$

where  $\Delta\theta = \theta' - \theta$ . In this expression the first term represents annihilation, the second one is the transmission contribution and the third one the reflection term. In general, the transition of the “in”-state

$$A_i(\theta_1) A_j(\theta_2) A_k(\theta_3)$$

to the “out”-state is not so simple. However, for integrable theories where one has a large quantity of conserved charges it happens that the existence of these charges imposes that, in every region where the particles are far away from each other, the wave function is a sum of plane waves where in each region the set of momenta  $\{p_i\}$  is the same. Then for these integrable theories we can obtain the “out”-state by applying (C.1) consecutively to the pairs in this triplet until the  $A$ ’s are ordered by decreasing rapidities. This is called factorizability. Now, consistency requires that the final result should not depend on whether we arrive at region  $\theta_3 < \theta_2 < \theta_1$  by scattering first  $A_j$  at first with either  $A_k$  or  $A_i$ . By doing it in both ways and equating both results one obtains for each choice of isospin indexes some constraint on the functions in (C.1). These equations can be obtained in a straightforward fashion and have a nice physical interpretation – see caption in figure 9 – all other possible choices of isovector indexes (i.e. colors) give rise either to the same constraints or to some trivial identities where the lhs

and the rhs are already identically equal. One obtains:

$$\begin{aligned} h(\theta) + h(\theta') &= h(\theta + \theta') \\ h(\theta) + g(\theta + \theta') &= g(\theta') \end{aligned} \quad (\text{C.2})$$

plus another similar, yet bigger, equation corresponding to the third identity in figure 9. The solution of the 2 equations yield  $h(\theta)$  and  $g(\theta)$  in terms of two constants  $\lambda$  and  $\kappa$ . When plugging these solutions into the third equation one obtains  $\kappa(\lambda)$ . At the end of the day one has

$$h(\theta) = g(i\lambda - \theta) = \frac{i\theta}{\lambda}. \quad (\text{C.3})$$

Thus, out of 3 functions we are now left with one function and one constant. From (C.1) one reads off the S-matrix

$$S_{ik}^{jl}(\theta) = S_2(\theta) [\delta_{ik}\delta_{jl}g^{-1}(\theta) + \delta_{ij}\delta_{lk} + \delta_{il}\delta_{jk}h^{-1}(\theta)] \quad (\text{C.4})$$

Changing  $i \leftrightarrow j$  and the channel  $s = 4m_0^2 \cosh^2(\pi\theta/2) \leftrightarrow u$  (i.e.  $\theta \rightarrow i - \theta$ ) should leave the S-matrix invariant. This is crossing-symmetry. It implies

$$S_2(\theta) = S_2(i - \theta) \quad (\text{C.5})$$

and  $h(\theta) = g(i - \theta)$ , or  $\lambda = 1$ . Finally we must impose the most natural requirement, namely, unitarity. Setting

$$S_{mn}^{jl}(-\theta)S_{ik}^{mn}(\theta) = \delta_{ij}\delta_{kl}S_2(-\theta)S_2(\theta)(1 + h^{-1}(-\theta)h^{-1}(\theta)) + \delta_{ik}\delta_{jl}(\dots) + \delta_{il}\delta_{kj}(\dots)$$

to be equal to  $\delta_{ij}\delta_{kl}$  one obtains 3 equations. The exact expressions inside the parentheses are not relevant for our discussion. It suffices to say that, for the  $g$  and  $h$  we found, (C.3), they vanish identically. Thus one is left with

$$S_2(-\theta)S_2(\theta) = \frac{\theta^2}{\theta^2 + 1}. \quad (\text{C.6})$$

From (C.5) and (C.6) it follows that  $S_2(\theta)$  is given by

$$\frac{\theta}{\theta - i}S_0^2(\theta), \quad S_0(\theta) = i \frac{\Gamma(-\frac{\theta}{2i})\Gamma(\frac{1}{2} + \frac{\theta}{2i})}{\Gamma(\frac{\theta}{2i})\Gamma(\frac{1}{2} - \frac{\theta}{2i})} \quad (\text{C.7})$$

times a CDD factor

$$f(\theta) = \prod_{k=1}^L \frac{\sinh \pi\theta + i \sin \alpha_k}{\sinh \pi\theta - i \sin \alpha_k} \quad (\text{C.8})$$

where  $\alpha_k$  are arbitrary real numbers. The form (C.7) is needed to have the right pole and zero structure according to (C.5) and (C.6) while the ambiguity (C.8) is unfixed since  $f(\theta)/f(i - \theta) = f(\theta)f(-\theta) = 1$ . Absence of additional bound states forces one not only to exclude this factor

but also to introduce the  $i$  in  $S_0(\theta)$  [43,77]. For the non-linear sigma model the correct S-matrix is indeed given by the minimal choice (C.7). To verify this claim some convincing cross checks are done [38,78]. Nevertheless notice that for what concerns the classical analysis we did not need to know anything about this CDD factor since for large  $\theta$ 's it is given by  $1 + \mathcal{O}(e^{-2\pi\theta})$  being therefore irrelevant in the scaling limit. If this CDD factor was present it could, however, in principle contribute into quasi-classical corrections.

Finally since  $SO(4) = SU(2) \times SU(2)$  we can replace  $i, k, j, l$  by  $(\alpha, \dot{\alpha}), (\beta, \dot{\beta}), (\alpha', \dot{\alpha}'), (\beta', \dot{\beta}')$  and write (C.4) as

$$\begin{aligned} & \frac{S_0^2(\theta)}{(\theta - i)^2} \left( i\theta \epsilon_{\alpha\beta} \epsilon_{\dot{\alpha}\dot{\beta}} \epsilon^{\alpha'\beta'} \epsilon^{\dot{\alpha}'\dot{\beta}'} + \theta(\theta - i) \delta_{\alpha}^{\alpha'} \delta_{\dot{\alpha}}^{\dot{\alpha}'} \delta_{\beta}^{\beta'} \delta_{\dot{\beta}}^{\dot{\beta}'} - i(\theta - i) \delta_{\alpha}^{\beta'} \delta_{\dot{\alpha}}^{\dot{\beta}'} \delta_{\beta}^{\alpha'} \delta_{\dot{\beta}}^{\dot{\alpha}'} \right) \\ &= \frac{S_0^2(\theta)}{(\theta - i)^2} \left( \theta \delta_{\alpha}^{\alpha'} \delta_{\beta}^{\beta'} - i \delta_{\alpha}^{\beta'} \delta_{\beta}^{\alpha'} \right) \left( \theta \delta_{\dot{\alpha}}^{\dot{\alpha}'} \delta_{\dot{\beta}}^{\dot{\beta}'} - i \delta_{\dot{\alpha}}^{\dot{\beta}'} \delta_{\dot{\beta}}^{\dot{\alpha}'} \right). \end{aligned}$$

or

$$\hat{S}(\theta) = \hat{S}_R(\theta) \times \hat{S}_L(\theta) \quad , \quad \hat{S}_{L,R}(\theta) = S_0(\theta) \hat{\mathcal{R}}(\theta) \quad , \quad \hat{\mathcal{R}} = \frac{\theta \hat{I} - i \hat{P}}{\theta - i} \quad (\text{C.9})$$

where  $\hat{P}$  is the permutation operator in  $\mathbb{C}^2 \times \mathbb{C}^2$ . Notice that, since  $SO(4) = SU(2) \times SU(2)$ , we could have started with this ansatz where

$$\hat{S}_{L,R}(\theta) = \hat{S}_0(\theta) \frac{\theta}{\theta - i} \left( \hat{I} - h^{-1}(\theta) \hat{P} \right) .$$

instead of starting with (C.1). The absence of the channel where two particles annihilate is natural since the particles are charged with left/right charge. Consistency relation would be represented by the first equation in figure 9 only, or equation (C.2), which states that  $h(\theta)$  is linear in  $\theta$ . Then we would continue by imposing unitarity and crossing-symmetry to arrive at the same results we did for the form of  $S_0$  and the proportionality constant in  $h(\theta)$ . The results of this appendix could be easily generalized to both  $O(N)$  and  $SU(N)_L \times SU(N)_R$  non-linear sigma models or to many other groups.

Let us now start from the obtained S-matrix (C.9) and carry out the algebraic Bethe ansatz program [71]. We introduce a ghost particle in the auxiliary space 0 and scatter it through the other particles. We want to diagonalize

$$\text{Tr} \hat{T}(\theta) \quad , \quad \hat{T}(\theta) = \prod_{k=1}^L \hat{S}_{0k}(\theta - \theta_k)$$

where we trace over the auxiliary space. This is a relevant problem because if we solve it for any  $\theta$  and then set  $\theta = \theta_k$  then this means that the ghost particle will change its quantum numbers with particle  $k$  since  $\hat{S}_{0k}(0) = -P_{0k} \times P_{0k}$ . In other words,

$$- \text{Tr} \hat{T}(\theta_k) = \hat{S}_{k,k-1}(\theta_k - \theta_{k-1}) \dots \hat{S}_{k,1}(\theta_k - \theta_1) \hat{S}_{k,N}(\theta_k - \theta_N) \dots \hat{S}_{k,k+1}(\theta_k - \theta_{k+1})$$

so that the problem of imposing periodicity of the wave function reads

$$- e^{im_0 \mathcal{L} \sinh(\pi\theta_k)} \text{Tr} \hat{T}(\theta_k) |\Psi\rangle = |\Psi\rangle . \quad (\text{C.10})$$

Let us now perform the diagonalization of C.10. We consider

$$|\Psi\rangle = \prod_{i=1}^{J_u} \hat{B}_L(u_i) \prod_{j=1}^{J_v} \hat{B}_R(v_j) |\Omega(\theta_1, \dots, \theta_L)\rangle \quad (\text{C.11})$$

where  $\Omega$  is the state with  $L$  particles, where the right and left spin of every particle is pointing in the up direction, and

$$\hat{T}_R(\theta) = \prod_{k=1}^L \hat{S}_{R,0k}(\theta - \theta_k) = \begin{pmatrix} \hat{A}_R(\theta) & \hat{B}_R(\theta) \\ \hat{C}_R(\theta) & \hat{D}_R(\theta) \end{pmatrix} \quad (\text{C.12})$$

with a similar definition for the left sector. Acting on  $\Omega$  one has

$$\mathcal{R}_{0k}(\theta) |\Omega\rangle = \frac{1}{\theta - i} \begin{pmatrix} \theta - \frac{i}{2}(\tau^3 + 1) & -\frac{i}{2}\tau^- \\ -\frac{i}{2}\tau^+ & \theta + \frac{i}{2}(\tau^3 - 1) \end{pmatrix} |\Omega\rangle = \frac{1}{\theta - i} \begin{pmatrix} (\theta - i) |\Omega\rangle & * \\ 0 & \theta |\Omega\rangle \end{pmatrix}$$

The upmost right element is not important for our discussion. However the vanishing of the element in the left down corner is. It implies that  $|\Omega\rangle$  is eigenvalue of both  $A$  and  $D$  with eigenvalues

$$\begin{aligned} A(\theta) |\Omega\rangle &= \prod_{\alpha=1}^L S_0(\theta - \theta_\alpha) |\Omega\rangle \\ D(\theta) |\Omega\rangle &= \prod_{\alpha=1}^L S_0(\theta - \theta_\alpha) \frac{\theta - \theta_\alpha}{\theta - \theta_\alpha - i} |\Omega\rangle \end{aligned}$$

So now we have to understand how  $A$  and  $D$  pass through the  $B$ 's. Consistency relations can be cast as  $S_{12}(\theta) S_{13}(\theta + \theta') S_{23}(\theta') = S_{23}(\theta') S_{13}(\theta + \theta') S_{12}(\theta)$  which imply (cf. [79])

$$T_{R,L}^a(\theta) T_{R,L}^{a'}(\theta') \mathcal{S}_{aa'}(\theta' - \theta) = \mathcal{S}_{aa'}(\theta' - \theta) T_{R,L}^{a'}(\theta') T_{R,L}^a(\theta).$$

where  $a$  and  $a'$  are two  $\mathbb{C}^2$  auxiliary spaces. This gives us the commutation relations between the elements of the transfer matrix (C.12). In particular

$$\begin{aligned} [B(\theta), B(\theta')] &= 0 \\ A(\theta) B(\theta') &= \frac{\theta' - \theta - i}{\theta' - \theta} B(\theta') A(\theta) + \frac{i}{\theta' - \theta} B(\theta) A(\theta') \end{aligned} \quad (\text{C.13})$$

$$D(\theta) B(\theta') = \frac{\theta' - \theta + i}{\theta' - \theta} B(\theta') D(\theta) - \frac{i}{\theta' - \theta} B(\theta) D(\theta'). \quad (\text{C.14})$$

for symbols in the same right or left sector. Symbols in different sectors commute to zero of course. Then, acting on (C.11), one has

$$\begin{aligned} -\text{Tr} \hat{T}(\theta) |\Psi\rangle &= (\hat{A}_R(\theta) + \hat{D}_R(\theta)) \times (\hat{A}_L(\theta) + \hat{D}_L(\theta)) \prod_{i=1}^{J_u} \hat{B}_L(u_i) \times \prod_{j=1}^{J_v} \hat{B}_R(v_j) |\Omega(\theta_1, \dots, \theta_L)\rangle \\ &= \prod_{\alpha=1}^L S_0^2(\theta - \theta_\alpha) \left( \prod_{i=1}^{J_u} \frac{u_i - \theta - i}{u_i - \theta} + \prod_{i=1}^{J_v} \frac{u_i - \theta + i}{u_i - \theta} \prod_{\alpha=1}^L \frac{\theta - \theta_\alpha}{\theta - \theta_\alpha - i} \right) \\ &\times \left( \prod_{i=1}^{J_v} \frac{v_i - \theta - i}{v_i - \theta} + \prod_{i=1}^{J_u} \frac{v_i - \theta + i}{v_i - \theta} \prod_{\alpha=1}^L \frac{\theta - \theta_\alpha}{\theta - \theta_\alpha - i} \right) |\Psi\rangle + \dots \end{aligned}$$

where dots stand for *undesirable* terms which would make  $|\Psi\rangle$  not to be an eigenvector of  $\text{Tr } \hat{T}$  while the displaced term is the one we obtain ignoring the second term in the rhs of both (C.13) and (C.14). The condition that these *undesirable* terms vanish gives us a set of equations for  $u_i$  and  $v_j$ . There is however a shortcut to arrive at these equations provided we know that these terms can indeed be killed. The argument is the following – each of the two last terms inside the big parentheses came from the diagonalization of a product of  $Q = \theta - iP$ . The diagonalization of such a product of operators must yield a polynomial in  $\theta$  therefore the residues of the apparent poles which seem to be part of the eigenvalue for  $\theta = u_i$  (or  $v_j$ ) must vanish. This implies

$$1 = \prod_{i \neq j}^{J_u} \frac{u_j - u_i + i}{u_j - u_i - i} \prod_{\alpha=1}^L \frac{u_j - \theta_\alpha}{u_j - \theta_\alpha + i} \quad (\text{C.15})$$

$$1 = \prod_{i \neq j}^{J_v} \frac{v_j - v_i + i}{v_j - v_i - i} \prod_{\alpha=1}^L \frac{v_j - \theta_\alpha}{u_j - \theta_\alpha + i} \quad (\text{C.16})$$

Furthermore (C.10) reads

$$e^{im_0 \mathcal{L} \sinh \pi \theta_\beta} \prod_{\alpha \neq \beta}^L S_0^2(\theta_\beta - \theta_\alpha) \prod_{i=1}^{J_u} \frac{\theta_\beta - u_i + i}{\theta_\beta - u_i} \prod_{i=1}^{J_v} \frac{\theta_\beta - v_i + i}{\theta_\beta - v_i} = 1. \quad (\text{C.17})$$

Equations (C.15-C.17) coincide precisely with (3.4-3.6) after the trivial shift  $(u, v) \rightarrow (u - i/2, v - i/2)$  in the former.

## Appendix D Bethe Ansatz Equations for $O(2n)$ Sigma-Model

Zamolodchikovs' S-matrix for the  $O(2n)$  sigma-model takes the form [38, 80]

$$\hat{S}_{a b}^{a' b'}(\theta) = \sigma_2(\theta) \left[ \hat{I}_{a b}^{a' b'} - \frac{i}{\theta} \hat{P}_{a b}^{a' b'} - \frac{i}{i(n-1) - \theta} \hat{K}_{a b}^{a' b'} \right] \quad (\text{D.1})$$

where the overall factor is given by

$$\sigma_2(\theta) = \frac{\Gamma(\Delta + \varphi) \Gamma(1 - \varphi) \Gamma(\frac{1}{2} + \varphi) \Gamma(\frac{1}{2} + \Delta - \varphi)}{\Gamma(1 + \Delta - \varphi) \Gamma(\varphi) \Gamma(\frac{1}{2} - \varphi) \Gamma(\frac{1}{2} + \Delta + \varphi)}, \quad (\text{D.2})$$

$$\varphi = \frac{-i\theta}{2n-2}, \quad \Delta = \frac{1}{2n-2}, \quad (\text{D.3})$$

and

$$\hat{I}_{a b}^{a' b'} = \delta_a^{a'} \delta_b^{b'}, \quad \hat{P}_{a b}^{a' b'} = \delta_a^{b'} \delta_b^{a'}, \quad \hat{K}_{a b}^{a' b'} = \delta_{ab} \delta^{a' b'} \quad (\text{D.4})$$

are  $O(2n)$ -invariant tensor bases. Let us restrict ourselves to  $n \geq 2$ . The above form is determined as a minimal solution satisfying the Yang-Baxter equation

$$\hat{S}_{c_1 c_2}^{b_1 b_2}(\theta) \hat{S}_{a_1 c_3}^{c_1 b_3}(\theta + \theta') \hat{S}_{a_2 a_3}^{c_2 c_3}(\theta') = \hat{S}_{a_1 a_2}^{c_1 c_2}(\theta) \hat{S}_{c_1 a_3}^{b_1 c_3}(\theta + \theta') \hat{S}_{c_2 c_3}^{b_2 b_3}(\theta'), \quad (\text{D.5})$$

the unitarity condition

$$\hat{S}_{b_1 b_2}^{c_1 c_2}(\theta) \hat{S}_{a_1 a_2}^{b_1 b_2}(-\theta) = \hat{I}_{a_1 a_2}^{c_1 c_2}, \quad (\text{D.6})$$

and the crossing symmetry

$$\hat{S}_{a'b'}^{a'b}(i(n-1)-\theta) = \hat{S}_{a'b'}^{a'b}(\theta). \quad (\text{D.7})$$

By non-trivial comparison with perturbation theory [38, 80–82], this S-matrix is believed to describe the scattering of vector particles in the  $O(2n)$  sigma-model. Let us consider the system of  $L$  particles put into a one-dimensional periodic box. The system is described by the Bethe wave function  $\psi^{a_1 \dots a_L}(\theta_1, \dots, \theta_L)$  where  $\{\theta_\alpha\}$  are rapidities associated with each of the particles. The wave function reflects the elastic, factorisable property of the scattering as

$$\psi^{b_2 b_1 a_3 \dots a_L}(\theta_2, \theta_1, \theta_3, \dots, \theta_L) = \hat{S}_{a_1 a_2}^{b_1 b_2}(\theta_1 - \theta_2) \psi^{a_1 a_2 a_3 \dots a_L}(\theta_1, \theta_2, \theta_3, \dots, \theta_L). \quad (\text{D.8})$$

It also satisfies the periodic boundary condition

$$\psi^{a_2 \dots a_L a_1}(\theta_2, \dots, \theta_L, \theta_1) = e^{-ip(\theta_1)} \psi^{a_1 \dots a_L}(\theta_1, \dots, \theta_L). \quad (\text{D.9})$$

The momentum of the  $i$ th particle is given by  $p(\theta_\alpha) = \mu \sinh(\frac{\pi}{n-1}\theta_\alpha)$ . Following from these properties, the wave function obeys the Yang equations

$$\left[ e^{-ip(\theta_\alpha)} (\delta_{a_1}^{b_1} \dots \delta_{a_L}^{b_L}) + \hat{T}(\theta_\alpha)_{a_1 \dots a_L}^{b_1 \dots b_L} \right] \psi^{a_1 \dots a_L}(\theta_1, \dots, \theta_L) = 0, \quad (\text{D.10})$$

for  $\alpha = 1, \dots, L$ . We introduced the transfer matrix  $\hat{T}(u)_{a_1 \dots a_L}^{b_1 \dots b_L}$ , given by the trace

$$\hat{T}(u)_{a_1 \dots a_L}^{b_1 \dots b_L} = \hat{\Omega}_a^a(u)_{a_1 \dots a_L}^{b_1 \dots b_L} \quad (\text{D.11})$$

where

$$\hat{\Omega}_a^b(u)_{a_1 \dots a_L}^{b_1 \dots b_L} = \hat{S}_{a_1 a_1}^{c_1 b_1}(u - \theta_1) \hat{S}_{c_1 a_2}^{c_2 b_2}(u - \theta_2) \dots \hat{S}_{c_L a_L}^{b_L}(u - \theta_L) \quad (\text{D.12})$$

is the monodromy matrix.

The matrix-valued equations (D.10) can be diagonalized with the help of the nested Bethe ansatz [71]. Supplied with an appropriately defined Bethe vector (wave function) [83], the transfer matrix  $\hat{T}(u)$  is diagonalized independently of the value of  $u$ . The lowest eigenvalue is given by

$$T(u) = W(u) \sum_{k=1}^n (t_k(u) + \bar{t}_k(u)), \quad (\text{D.13})$$

where

$$\begin{aligned} t_k(u) &= Y_{k-1}\left(u - \frac{ki}{2}\right)^{-1} Y_k\left(u - \frac{(k-1)i}{2}\right), \quad \text{for } k = 1, \dots, n-2, \\ t_{n-1}(u) &= Y_{n-2}\left(u - \frac{(n-1)i}{2}\right)^{-1} Y_{n-1}\left(u - \frac{(n-2)i}{2}\right) Y_n\left(u - \frac{(n-2)i}{2}\right), \\ t_n(u) &= Y_{n-1}\left(u - \frac{ni}{2}\right)^{-1} Y_n\left(u - \frac{(n-2)i}{2}\right), \\ \bar{t}_k(u) &= Y_{k-1}\left(u - \frac{(2n-2-k)i}{2}\right) Y_k\left(u - \frac{(2n-1-k)i}{2}\right)^{-1}, \quad \text{for } k = 1, \dots, n-2, \\ \bar{t}_{n-1}(u) &= Y_{n-2}\left(u - \frac{(n-1)i}{2}\right) Y_{n-1}\left(u - \frac{ni}{2}\right)^{-1} Y_n\left(u - \frac{ni}{2}\right)^{-1}, \\ \bar{t}_n(u) &= Y_{n-1}\left(u - \frac{(n-2)i}{2}\right) Y_n\left(u - \frac{ni}{2}\right)^{-1}. \end{aligned} \quad (\text{D.14})$$

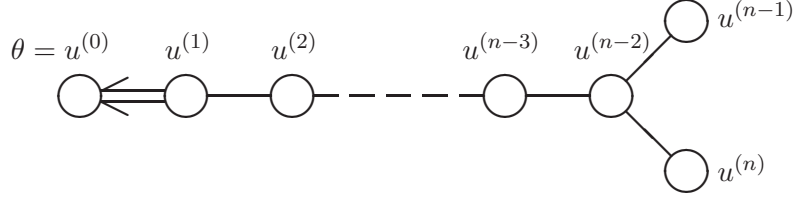


Figure 10: Dynkin diagram for the  $B_n^{(1)}$  root system

Scattering terms  $W(u), Y_k(u)$  are defined as

$$W(u) = \prod_{\alpha=1}^{K_0} \sigma_2(u - u_\alpha^{(0)}), \quad (\text{D.15})$$

$$Y_k(u) = \prod_{j=1}^{K_k} \frac{u - u_j^{(k)} + \frac{i}{2}}{u - u_j^{(k)} - \frac{i}{2}}, \quad \text{for } k = 0, \dots, n. \quad (\text{D.16})$$

We sometimes use the notations  $u_\alpha^{(0)} := \theta_\alpha$  and  $K_0 := L$  for the sake of simplicity.  $\{u_j^{(k)}\}$  are rapidities of magnons introduced in the construction of the Bethe vector [83].

The diagonalized Yang equations are then given by

$$e^{-i\mu \sinh(\frac{\pi}{n-1}\theta_\alpha)} = \prod_{\beta \neq \alpha}^L S_0(\theta_\alpha - \theta_\beta) \prod_{j=1}^{K_1} \frac{\theta_\alpha - u_j^{(1)} + \frac{i}{2}}{\theta_\alpha - u_j^{(1)} - \frac{i}{2}}, \quad (\text{D.17})$$

$$S_0(\theta) = \frac{\theta - i}{\theta} \sigma_2(\theta) = -\frac{\Gamma(\Delta + \varphi)\Gamma(1 - \varphi)\Gamma(\frac{1}{2} + \varphi)\Gamma(\frac{1}{2} + \Delta - \varphi)}{\Gamma(\Delta - \varphi)\Gamma(1 + \varphi)\Gamma(\frac{1}{2} - \varphi)\Gamma(\frac{1}{2} + \Delta + \varphi)}. \quad (\text{D.18})$$

To make the diagonalization complete, the rapidities  $\{u_j^{(k)}\}$  have to satisfy the Bethe ansatz equations. Ignoring the common scalar factor  $W(u)$ ,  $T(u)$  is essentially a polynomial in  $u$  by construction and thus has no pole at any finite value of  $u$ . The requirement of cancellation of poles between two consecutive terms in  $T(u)$  gives rise to the Bethe ansatz equations

$$-1 = \prod_{l=0}^n \prod_{j=1}^{K_l} \frac{u_i^{(k)} - u_j^{(l)} + \frac{i}{2}(\alpha_k|\alpha_l)}{u_i^{(k)} - u_j^{(l)} - \frac{i}{2}(\alpha_k|\alpha_l)}. \quad (\text{D.19})$$

$\{\alpha_k\}$  ( $k = 1, \dots, n$ ) denote the simple roots of the  $D_n = \mathfrak{so}(2n)$  Lie algebra and  $(\alpha_k|\alpha_l)$  expresses inner product defined in the root space. The non-zero elements read explicitly  $(\alpha_k|\alpha_k) = 2$  ( $k = 1, \dots, n$ ),  $(\alpha_k|\alpha_{k+1}) = -1$  ( $k = 1, \dots, n-2$ ) and  $(\alpha_{n-2}|\alpha_n) = -1$ , which are encoded in the Dynkin diagram (see Fig.10). In addition we formally introduced an extra root  $\alpha_0$  giving  $(\alpha_0|\alpha_k) = -\delta_{1k}$ , so that the interaction between  $\theta_\alpha$ 's and  $u_j^{(k)}$ 's are included in the common notation (D.19). Note that the norm of  $\alpha_0$  can be fixed as  $(\alpha_0|\alpha_0) = 1$ , if we take account of the asymptotics of the self interaction between  $\theta_\alpha$ 's: Observing the asymptotics

$$S_0(\theta) = 1 - \frac{i}{\theta} + \mathcal{O}(\theta^{-2}), \quad (\text{D.20})$$



we see that the self interaction between  $\theta_\alpha$ 's is half the strength of that of  $u_i$ 's. In the Sutherland limit, the Yang equation (D.17) and the Bethe ansatz equations (D.19) are unified into the form

$$\sum_{l=0}^n (\alpha_k | \alpha_l) \mathcal{G}_l(u_i^{(k)}/M) = 2\pi n_i^{(k)}, \quad \text{for } k = 0, \dots, n, \quad (\text{D.21})$$

with mode numbers  $n_i^{(k)} \in \mathbb{Z}$  and resolvents

$$G_k(z) = \frac{1}{M} \sum_{j=1}^{K_k} \frac{1}{z - u_j^{(k)}/M}. \quad (\text{D.22})$$

Note that  $\alpha_0$  precisely corresponds to the affine root which extends the root system of  $D_n$  to that of the  $B_n^{(1)}$  affine Lie algebra. This enhanced symmetry may be viewed as a part of the symmetry of the conformal field theory arising at the renormalization fixed point.

## References

- [1] J. M. Maldacena, Adv. Theor. Math. Phys. **2** (1998) 231 [Int. J. Theor. Phys. **38** (1999) 1113] [arXiv:hep-th/9711200].
- [2] E. Witten, Adv. Theor. Math. Phys. **2** (1998) 253 [arXiv:hep-th/9802150].
- [3] S. S. Gubser, I. R. Klebanov and A. M. Polyakov, Phys. Lett. B **428** (1998) 105 [arXiv:hep-th/9802109].
- [4] O. Aharony, S. S. Gubser, J. M. Maldacena, H. Ooguri and Y. Oz, Phys. Rept. **323** (2000) 183 [arXiv:hep-th/9905111].
- [5] R. R. Metsaev and A. A. Tseytlin, Nucl. Phys. B **533** (1998) 109 [arXiv:hep-th/9805028].
- [6] J. A. Minahan and K. Zarembo, JHEP **0303** (2003) 013 [arXiv:hep-th/0212208].
- [7] L. N. Lipatov, JETP Lett. **59**, 596 (1994), hep-th/9311037.
- [8] L. D. Faddeev and G. P. Korchemsky, Phys. Lett. **B342**, 311 (1995), hep-th/9404173.
- [9] I. Bena, J. Polchinski and R. Roiban, Phys. Rev. D **69** (2004) 046002 [arXiv:hep-th/0305116].
- [10] S. S. Gubser, I. R. Klebanov and A. M. Polyakov, Nucl. Phys. B **636** (2002) 99 [arXiv:hep-th/0204051].
- [11] S. Frolov and A. A. Tseytlin, JHEP **0206** (2002) 007 [arXiv:hep-th/0204226].
- [12] S. Frolov and A. A. Tseytlin, Nucl. Phys. B **668** (2003) 77 [arXiv:hep-th/0304255].
- [13] N. Beisert, C. Kristjansen and M. Staudacher, Nucl. Phys. B **664** (2003) 131 [arXiv:hep-th/0303060].
- [14] N. Beisert, Nucl. Phys. B **682** (2004) 487 [arXiv:hep-th/0310252].
- [15] N. Beisert and M. Staudacher, Nucl. Phys. B **670** (2003) 439 [arXiv:hep-th/0307042].
- [16] B. Sutherland, Phys. Rev. Lett. **74**, 816 (1995).
- [17] B. S. Shastry and A. Dhar J. Phys. A: Math. Gen. **34** (2001) 6197. [arxiv:cond-mat/0101464]

- [18] N. Beisert, J. A. Minahan, M. Staudacher and K. Zarembo, *JHEP* **0309** (2003) 010 [arXiv:hep-th/0306139].
- [19] V. A. Kazakov, A. Marshakov, J. A. Minahan and K. Zarembo, *JHEP* **0405** (2004) 024 [arXiv:hep-th/0402207].
- [20] V. A. Kazakov and K. Zarembo, *JHEP* **0410** (2004) 060 [arXiv:hep-th/0410105].
- [21] N. Beisert, V. A. Kazakov and K. Sakai, arXiv:hep-th/0410253.
- [22] N. Beisert, V. A. Kazakov, K. Sakai and K. Zarembo, arXiv:hep-th/0502226.
- [23] S. Schafer-Nameki, *Nucl. Phys. B* **714** (2005) 3 [arXiv:hep-th/0412254].
- [24] N. Beisert, V. A. Kazakov, K. Sakai and K. Zarembo, *JHEP* **0507** (2005) 030 [arXiv:hep-th/0503200].
- [25] M. Staudacher, “The factorized S-matrix of CFT/AdS,” *JHEP* **0505** (2005) 054 [arXiv:hep-th/0412188].
- [26] N. Beisert, V. Dippel and M. Staudacher, *JHEP* **0407** (2004) 075 [arXiv:hep-th/0405001].
- [27] N. Beisert and M. Staudacher, *Nucl. Phys. B* **727** (2005) 1 [arXiv:hep-th/0504190].
- [28] D. Serban and M. Staudacher, *JHEP* **0406** (2004) 001 [arXiv:hep-th/0401057].
- [29] S. Frolov and A. A. Tseytlin, *JHEP* **0307** (2003) 016 [arXiv:hep-th/0306130].
- [30] A. Parnachev and A. V. Ryzhov, *JHEP* **0210** (2002) 066 [arXiv:hep-th/0208010].
- [31] C. G. . Callan, H. K. Lee, T. McLoughlin, J. H. Schwarz, I. J. Swanson and X. Wu, *Nucl. Phys. B* **673**, 3 (2003) [arXiv:hep-th/0307032].
- [32] H. Fuji and Y. Satoh, arXiv:hep-th/0504123.
- [33] N. Beisert, A. A. Tseytlin and K. Zarembo, *Nucl. Phys. B* **715** (2005) 190 [arXiv:hep-th/0502173].
- [34] R. Hernandez, E. Lopez, A. Perianez and G. Sierra, *JHEP* **0506**, 011 (2005) [arXiv:hep-th/0502188].
- [35] N. Beisert and L. Freyhult, *Phys. Lett. B* **622** (2005) 343 [arXiv:hep-th/0506243].
- [36] N. Gromov and V. Kazakov, *Nucl. Phys. B* **736** (2006) 199 [arXiv:hep-th/0510194].
- [37] A. M. Polyakov, arXiv:hep-th/0512310.
- [38] A. B. Zamolodchikov and A. B. Zamolodchikov, *Nucl. Phys. B* **133** (1978) 525 [*JETP Lett.* **26** (1977) 457].
- [39] A. M. Polyakov and P. B. Wiegmann, *Phys. Lett. B* **131**, 121 (1983).
- [40] P. Wiegmann, *Phys. Lett. B* **142**, 173 (1984).
- [41] P. B. Wiegmann, *Phys. Lett. B* **141**, 217 (1984).
- [42] L. D. Faddeev and N. Y. Reshetikhin, *Annals Phys.* **167**, 227 (1986).
- [43] E. Ogievetsky, N. Reshetikhin and P. Wiegmann, *NORDITA-84/38*
- [44] P. B. Wiegmann, *JETP Lett.* **39** (1984) 214 [*Pisma Zh. Eksp. Teor. Fiz.* **39** (1984) 180].
- [45] V. A. Fateev, V. A. Kazakov and P. B. Wiegmann, *Nucl. Phys. B* **424**, 505 (1994) [arXiv:hep-th/9403099].

- [46] R. Shankar and E. Witten, Phys. Rev. D **17** (1978) 2134.
- [47] H. Saleur and B. Wehefritz-Kaufmann, Nucl. Phys. B **628** (2002) 407 [arXiv:hep-th/0112095].
- [48] N. Mann and J. Polchinski, arXiv:hep-th/0408162.
- [49] H. Dorn and H. J. Otto, Nucl. Phys. B **429**, 375 (1994) [arXiv:hep-th/9403141].
- [50] A. B. Zamolodchikov and A. B. Zamolodchikov, Nucl. Phys. B **477** (1996) 577 [arXiv:hep-th/9506136].
- [51] J. Teschner, Nucl. Phys. B **546**, 390 (1999) [arXiv:hep-th/9712256].
- [52] V. Fateev, Al. Zamolodchikov and A. Zamolodchikov, unpublished (see in P. Baseilhac and V. A. Fateev, Nucl. Phys. B **532**, 567 (1998) [arXiv:hep-th/9906010]).
- [53] A. M. Polyakov, Int. J. Mod. Phys. A **14** (1999) 645 [arXiv:hep-th/9809057].
- [54] V. A. Kazakov and A. A. Migdal, Nucl. Phys. B **311**, 171 (1988).
- [55] V. Kazakov, I. K. Kostov and D. Kutasov, Nucl. Phys. B **622**, 141 (2002) [arXiv:hep-th/0101011].
- [56] J. M. Maldacena, *Prepared for Theoretical Advanced Study Institute in Elementary Particle Physics (TASI 2002): Particle Physics and Cosmology: The Quest for Physics Beyond the Standard Model(s), Boulder, Colorado, 2-28 Jun 2002*
- [57] G. Arutyunov, S. Frolov and M. Staudacher, JHEP **0410** (2004) 016 [arXiv:hep-th/0406256].
- [58] G. Arutyunov, S. Frolov and M. Staudacher, JHEP **0410**, 016 (2004) [arXiv:hep-th/0406256].
- [59] S. Schafer-Nameki, M. Zamaklar and K. Zarembo, arXiv:hep-th/0507189.
- [60] S. Frolov, J. Plefka and M. Zamaklar, arXiv:hep-th/0603008.
- [61] L. D. Faddeev, E. K. Sklyanin and L. A. Takhtajan, Theor. Math. Phys. **40**, 688 (1980) [Teor. Mat. Fiz. **40**, 194 (1979)].
- [62] P. P. Kulish, N. Y. Reshetikhin and E. K. Sklyanin, Lett. Math. Phys. **5**, 393 (1981).
- [63] N. Beisert, arXiv:hep-th/0511082.
- [64] N. Mann and J. Polchinski, Phys. Rev. D **72** (2005) 086002 [arXiv:hep-th/0508232].
- [65] A. Rej, D. Serban and M. Staudacher, arXiv:hep-th/0512077.
- [66] N. Dorey and B. Vicedo, arXiv:hep-th/0601194.
- [67] S. Novikov, S. V. Manakov, L. P. Pitaevsky and V. E. Zakharov, “*Theory Of Solitons. The Inverse Scattering Method,*”
- [68] N. E. Zhukovsky, Trudi Otdelenia fizicheskikh nauk O.L.E., t.XIII, vip.2 (1906) (In Russian).
- [69] J. A. Minahan, Fortsch. Phys. **53**, 828 (2005) [arXiv:hep-th/0503143].
- [70] M. B. Green and J. H. Schwarz, Phys. Lett. B **109** (1982) 444.
- [71] A. B. Zamolodchikov and A. B. Zamolodchikov, Nucl. Phys. B **379** (1992) 602.
- [72] D. Berenstein, J. M. Maldacena and H. Nastase, JHEP **0204** (2002) 013 [arXiv:hep-th/0202021].
- [73] R. Kedem, T. R. Klassen, B. M. McCoy and E. Melzer, Phys. Lett. B **304** (1993) 263 [arXiv:hep-th/9211102].
- [74] A. Kuniba, T. Nakanishi and J. Suzuki, Mod. Phys. Lett. A **8** (1993) 1649 [arXiv:hep-th/9301018].

- [75] F. A. Smirnov, arXiv:hep-th/9802132.
- [76] T. Klose and K. Zarembo, to appear.
- [77] M. Karowski, Nucl. Phys. B **153** (1979) 244.
- [78] B. Berg, M. Karowski, V. Kurak and P. Weisz, Phys. Lett. B **76** (1978) 502.
- [79] L. D. Faddeev, arXiv:hep-th/9605187.
- [80] A. B. Zamolodchikov and A. B. Zamolodchikov, Annals Phys. **120** (1979) 253.
- [81] P. Hasenfratz, M. Maggiore and F. Niedermayer, Phys. Lett. B **245** (1990) 522.
- [82] P. Hasenfratz and F. Niedermayer, Phys. Lett. B **245** (1990) 529.
- [83] H. J. de Vega and M. Karowski, Nucl. Phys. B **280** (1987) 225.